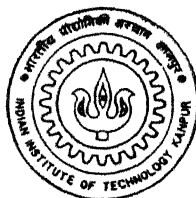


# PACKAGE DESIGN FOR A LOW COST OPTICAL LIQUID LEVEL SENSOR

by

Major Navjot Singh Bedi



TH  
EE/1999/M  
B39 p

DEPARTMENT OF ELECTRICAL ENGINEERING

**Indian Institute of Technology, Kanpur**

FEBRUARY, 1999

**PACKAGE DESIGN**  
**FOR**  
**A LOW COST OPTICAL LIQUID LEVEL**  
**SENSOR**

A Thesis Submitted  
in Partial Fulfilment of the Requirements  
for the Degree of  
**MASTER OF TECHNOLOGY**

**BY**  
**MAJOR NAVJOT SINGH BEDI**

to the  
DEPARTMENT OF ELECTRICAL ENGINEERING  
I.I.T KANPUR  
FEBURARY 1999

01 APR 1999 IEE

EE  
BEP

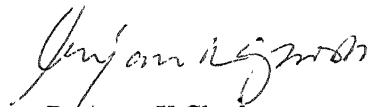
127828



A127828

## **CERTIFICATE**

It is certified that the work contained in the thesis entitled "PACKAGE DESIGN FOR A LOW COST OPTICAL LIQUID LEVEL SENSOR" by Major Navjot Singh Bedi, has been carried out under my supervision and this work has not been submitted elsewhere for a degree.



Dr Anjan K Ghosh

Professor

Electrical Engineering Deptt

I.I.T Kanpur

### **ACKNOWLEDGEMENTS**

I am extremely thankful to my thesis supervisor Dr Anjan K. Ghosh for not only introducing me to the interesting field of optical sensors and for giving me an opportunity to work in this field I also wish to place on record my gratitude for the continuous support, valuable guidance and words of encouragement, that I received during my stay at I.I.T Kanpur.

I am extremely thankful to my colleagues, Major's Anurag Chandra and T.S. Bains for making my stay memorable in the campus. A special word of thanks to Shailesh Tiwari, Ashish Patni, Maj Kamesh Kumar and S Vali Babu for their continuous support during this thesis work.

I am deeply indebted to my wife Geetika and daughter Lavanya, who stood by me and supported me all through the course, especially more so towards the end of the course.

Last but not the least , I am thankful to my erstwhile commanding officer, Colonel P.K.Bhatia, for providing me the time to study , because of which I got selected to do M.Tech at the premier institute of the country.

## **ABSTRACT**

Sensors are also the key components in condition monitoring and measurement systems which are important for automation. Optical sensors are increasingly becoming popular over the conventional measuring devices due to the possibility of non contact methods of measurement and the ability to reach inaccessible places when used in conjunction with optical fibres. Sensors are also the key components in condition monitoring and measurement systems which are important for automation. There is a need for an optical sensor design and development in India. The optical sensor design has to be cost effective for it to be acceptable to the Indian market. We have analysed various components of a low cost optical liquid level sensor using geometric optic and physical optic considerations and proposed a feasible design for the optical sensor. The detailed analysis of this sensor has been carried out in this thesis and guidelines for parameter selection have been evolved. The design guidelines of an optical liquid level sensor which uses an annular ring shaped detector has been proposed and its response has also been analysed in this thesis.

## **CONTENTS**

<b>1.</b>	<b>INTRODUCTION.....</b>	<b>1</b>
1 1	Optical Sensors . .	1
1 2	Overview of Research Work Done ..	3
1.3	Overview of Thesis .	4
	References . . .	5
<b>2.</b>	<b>OPTICAL SENSORS.....</b>	<b>8</b>
2.1	Types of Optical Sensors . .	8
2.2	Package Design For an Optical Sensor .. .	9
	References .	11
<b>3.</b>	<b>LIQUID LEVEL SENSORS.....</b>	<b>13</b>
3 1	Various Types of Liquid Level Sensors	13
3.2	A Simple Liquid Level Optic Sensor for a Case Study in Package Design	15
	References . . . . .	17
<b>4</b>	<b>GEOMETRIC OPTIC APPROACH FOR STUDY OF OPTICAL LIQUID LEVEL ARCHITECTURE.....</b>	<b>22</b>
4 1	Data Used for Generation of Results . . .	22
4.2	Beam Divergence Angle . ..	23
4 3	Half Divergence Angle Relationships and Results .	24
4 3 1	Analysis of Sensor Configuration No 1 ... .	24
4 3 2	Analysis of Sensor Configuration No 2 ... .	25
4 3 3	Analysis of Sensor Configuration No 3 .	26

4 3 4	Analysis of Sensor Configuration No 4	26
4 4	Comparative Analysis of the results obtained from all 4 topologies	27
4 5	Parameter Selection and Selection of type of Source.	27
4 6	Summary	28
	References	29
<b>5</b>	<b>WAVE PROPAGATION ANALYSIS. ....</b>	<b>37</b>
5 1	Shape of Liquid Meniscus .	37
5 2	Gaussian Beam Propagation.	38
5 3	Power Coupled to Photodiode	39
5 3 1	Power Coupled to Photodiode in an Offseted Detector	41
5 4	Expression for Spot Size for Sensor Configuration No 1	42
5 5	Expression for Spot Size for Sensor Configuration No 2	44
5 5 1	Total Internal Reflection Considerations for Configuration No 2	45
5 6	Expression for Spot Size for Sensor Configuration No 3	47
5 7	Expression for Spot Size for Sensor Configuration No 4	48
5 8	Summary	48
	References	49
<b>6.</b>	<b>SIMULATION RESULTS.....</b>	<b>59</b>
6 1	Analysis of Results	59
6 1 1	Test Data Used	59
6 1 2	Variation in Power and Coupling Efficiency	61
6 2	Selection of Feasible Design For an Optical Sensor	62
6 3	Effect of Variation in Design Parameters	64
6 4	Annular Detector based Optical Sensor	66
6 5	Responsivity and Dead Zone of Annular Detector	67
6 6	Reduction Of the effect of Offset	68

<b>7.</b>	<b>FUTURE WORK and CONCLUSIONS.....</b>	<b>81</b>
7 1	Conclusions	81
7 2	Scope for Future Work	81
7 2 1	Various Applications Possible	83
7 2 2	A Fibre Optic Liquid Level Sensor	83
	<b>APPENDICES.....</b>	<b>84</b>
A	Spot Size at detector for Sensor Configuration No 1.	84
B	Ray Matrix for a Concave Dielectric Interface...	86

## LIST OF TABLES

1 1	Advantages of Optical Sensors	6
1 2	Technological Applications Enhanced by the use of Optical Sensors	6
4 1	Value of Half Beam Divergence Angle for Sensor Configuration No 1	30
4 2	Value of Half Beam Divergence Angle for Sensor Configuration No 2	30
4 3	Value of Half Beam Divergence Angle for Sensor Configuration No 3	31
4 4	Value of Half Beam Divergence Angle for Sensor Configuration No 4	31
4 5	Comparative Analysis of min and max Values of Half Beam Divergence Angle for all the four Configurations	32
5 1	Variation in far field $z \gg (\pi w_0^2 n / \lambda)$ for various values of $w_0$ and $\lambda$	50
5 2	Variation in Half Beam Angle for various values of $w_0$ and $\lambda$	50
6 1	List of Design Parameters Selected	70

## LIST OF FIGURES

1 1	Smart Skin structures used in aircraft	7
2 1	A Simple Intensity Modulated Sensor	12
2 2	A Michelson Interferometer using bulk optic components	12
3 1	Float type of liquid level sensor	18
3 2	Capacitive type of liquid level sensor	18
3 3	An Ultrasound liquid level sensor	19
3 4	An Optic liquid level sensor	19
3 5	Optical Sensor Configuration No 1	20
3 6	Optical Sensor Configuration No 2	20
3 7	Optical Sensor Configuration No 3	21
3 8	Optical Sensor Configuration No 4	21
4 1	Set up for Geometric Optic Analysis of Configuration No 1	33
4 2	Set up for Geometric Optic Analysis of Configuration No 2	34
4 3	Set up for Geometric Optic Analysis of Configuration No 3	35
4 4	Set up for Geometric Optic Analysis of Configuration No 4	36
5 1	Radius of Curvature of a Liquid Surface	51
5 2	Smallest order of Gaussian Beam diverging away from its waist	52
5 3	The detector at an offset from the source	53
5 4	Spot size analysis for Configuration No 1	54
5 5	Schematic for analysis of Configuration No 2	55
5 6	Analysis of Total Internal Reflection condition for Configuration No 2	56
5 7	Schematic for analysis of Configuration No 3	57
5 8	Schematic for analysis of Configuration No 4	58
6 1	Coupling Efficiency vs Liquid level for Configuration No 1	71
6.2	Coupling Efficiency vs Liquid level for Configuration No 2	72
6 3	Coupling Efficiency vs Liquid level for Configuration No 3	73

6 4	Coupling Efficiency vs Liquid level for Configuration No 3. for offset variation	74
6 5	Coupling Efficiency vs Liquid level for Configuration No 3. (detector radius variation)	75
6 6	Efficiency vs Liquid level for Configuration No 3, for variation. in min spot size	76
6 7	Efficiency vs Liq level for Configuration No 3, for variation in refractive index.	77
6 8	Efficiency vs Liq level for Configuration No 3, for variation. in tube dia. .	78
6 9	Schematic of an Annular Detector	79
6 10	Coupling Efficiency vs Liquid level for an Annular Detector ..	80
A 1	Concave Spherical Dielectric Interface	88

## **CHAPTER 1**

### **INTRODUCTION**

A sensor is a device which converts a change in one physical parameter, into a change in the magnitude or phase of a second, different parameter, which can be measured more conveniently and perhaps more accurately [1] Sensors are used for measurement, detection, communication or provisioning of control signal to various parts or process of a system [2]

Condition monitoring and measurement systems are important for automation, which is critical in modern technology Sensors are key components in these systems As the push towards automation continues, the design and development of sensors is growing

#### **1.1 Optical Sensors**

Optical technologies have long played an important role in instrumentation and sensors, especially for non-contact measurements In an optical sensor, the information is passed from the physical /chemical variable being measured to an optical beam The changes in the characteristics of the optical beam are then determined Due to this structure, optical sensors have several advantages, which are listed in table 1 1

The optical sensors have enhanced and improved upon many existing applications, which are listed in table 1 2, and have also enabled some new applications to become possible One example of such a new application is monitoring the condition of critical structural parts such as bridge, trusses and aircraft skins Structures equipped with optical sensors to monitor their internal conditions during fabrication and operation are termed as smart structures and smart skins [2] Fig 1 1 illustrates schematically how an array of fibre optic gauges in an aircraft wing might provide a real time approximation to the actual strain distribution in the wing The goal of smart structure and smart skin research is to provide sufficient

information on conditions within critical structural systems so that corrective action can be taken in time to avoid a catastrophic failure such as rupture or buckling

In the developed nations of the world, optical sensor industry is a multi million dollar business and is projected to grow into a 560 million dollar industry by the turn of the century [3] Yet in India, optical sensors represent an emerging field. Most of the optical components are generally imported which makes them costly. Thus, there is a need for optical sensor design and development. The optical sensor design should be cost effective for it to be acceptable to the Indian market. Once a market for indigenous optical sensors is established we can think in terms of expensive optical sensors

In general optical sensors consist of (a) Optical Sources (b) Sensing elements through which/ in which the physical or chemical variables and optical fields interact (c) Photodetector (d) Electronic circuitry for signal processing and display [4] The components (a) - (d) are combined in a package

The performance of an optical sensor depends on the relative placement of all mechanical and electrical components into a package. For an optical sensor desired to be cost effective and simple, it should comprise of the fewest possible number of optical components and a simple low cost package. A package has many other roles in determining the overall performance of a sensor, such as

**(a). Alignment** The alignment of all optical, opto mechanical and opto electronic components and maintenance of the initial alignment throughout the life of the sensor is a critical aspect of packaging of optical sensors

**(b). Thermal Stability** Ensuring thermal stability of all components of an optical sensor is determined by the package design.

**(c). Shielding from Stray Radiation's** Shielding from both optical and RF or EMI radiation's, is done by the package, and the components inside the package are thus not affected by stray radiation's

(d). **Spacing.** Spacing between the source and detector needs to be maintained properly. The focus of our attention in this thesis is how to select the interelement spacing in a sensor package. We study the effect of spacing variation on the output of the sensor.

While considering spacing, we take into account the relative importance of the size of the source and detector in the package and the overall arrangement of these items. We observe how the output of the sensor varies with parameters related to spacing and sizes and the arrangements.

## 1.2 Overview of Research Work Done

A low cost optical liquid level sensor that can be easily fabricated has been proposed and the possible topologies to implement such a sensor have been analysed. The proposed sensor is simple in design and consists of only a source, a detector, a physical variable and a tubular package to keep everything in it. This type of liquid level sensors can be used in the automobile industry, in the aeronautical industry and in measurement of the level of oil in electrical transformers (where electrical sensors can't be used).

The following design objectives have been looked at:

- (a) The relative importance of the size of the source and detector on the output of the sensor.
- (b) The effect of the variation in various dimensions of the package design, on the output of the sensor.
- (c) The effect of variation in the power and spot size of the beam emitted by the source, on the output of the sensor.

While carrying out the analysis of the optic sensor using geometric optics approach, it is assumed that a plane wave of light, coming from a point source falls on a plane mirror like liquid surface and undergoes reflection / refraction. The transcendental equations relating the half acceptance angle, with other known parameters were derived for each topology, assuming that no side wall reflections take place. We developed guidelines for parameter selection for the type of source, to be used in our set-up, given all other dimensions.

The second approach followed in the analysis was based on wave propagation & diffraction. The light beam was considered to be gaussian in nature, which is a reasonable approximation for a narrow, monochromatic, directional beam of light. The radius of curvature of the liquid surface in the sensor tube was incorporated in the calculations. Using this analysis all the parameters related to spacing and size for the different arrangements were derived. Lateral offset between the source and detector was also considered in the design where applicable. We found that a reflective optical sensor arrangement with a source and an adjacent photodetector is the most practical for implementation in this design. In this design the coupling efficiency can vary between 6% to 14 % if the photodetector size is twice that of the source spot size. In this type of a liquid level sensor there is a maxima in the coupling efficiency as the function of the liquid level. We can carry out level measurements either in the linear ranges before the maxima or after the maxima. A design for an optical sensor which uses the annular (ring shaped) detector has been proposed and it is seen that there is no requirement of catering for an offset in such a detector. This type of detector is also unaffected by misalignments caused due to a tilt in the tube.

### 1.3 Overview of Thesis

In chapter 2, we have looked closely at optical sensors and the importance of package design. The various types of optical sensors and their advantages have also been listed.

Chapter 3 pertains to liquid level sensors and the need for such sensors has been touched upon. Various optical sensors for level sensing are also discussed. The four possible topologies of our low cost simple optical sensor for liquid level measurement are discussed in this chapter.

Chapter 4 deals with the geometric optics approach in the analysis of our optical sensor design and this analysis primarily helped in selection of the type of source to be used. As few inferences could be drawn from this approach, the analysis was done using the plane wave propagation approach.

In chapter 5, the analysis of our optical sensor design has been carried out using wave propagation approach. All the four proposed topologies of our low cost simple optical sensor for liquid measurement have been analysed and expressions for the spot size and power at the detector in each configuration have been derived. In case of the reflective type of sensor configurations, the offset between the source and the detector has also been taken into account.

Chapter 6 pertains to the analysis of all the four configurations of the optical sensor and selection of a feasible design for our low cost optical liquid level sensor. Then using this feasible design which has been selected, further analysis of our optical sensor, using this feasible design, which has been selected is done. A package design for an 'annular ring' shaped detector base optical sensor is also proposed.

In chapter 7, scope for further work has been elaborated & conclusions for the work done in the thesis have been drawn. The scope for utilising the work done in this thesis, in fields other than liquid level sensing has also been touched upon.

## REFERENCES

- [1] J P Dakin, "Optical Fibre Sensors ", summer school on " Principles of Optical Systems ", held at Rose Priori, organised by Strathclyde University, Glasgow, 1987
- [2] A B Buckman, " Guided -Wave Photonics ", Saunders College Publishing, New York, 1996, Chapter 9
- [3] B P Pal (Ed), "Fundamentals of Fibre Optics in Telecommunications and Sensor Systems", Wiley Eastern, New Delhi, 1992, Chapter 22
- [4] A K Ghosh and P K Paul, " Alignment Considerations in Extrinsic Fibre Optic Sensors ", Applied Optics, Vol 36 1997, pp 6256 - 6263

**TABLE 1.1**

**ADVANTAGES OF OPTICAL SENSORS**

- 1 Predominantly dielectric construction so it can be used in high voltage , electrically noisy, high temperature , corrosive and other stressing environments Also , immunity of the signal to EMI / RFI
- 2 Highly reliable and safe with no risk of arcing
- 3 No residual capacitive or inductive effect
- 4 Small size and weight
- 5 Allows access to normally inaccessible areas when used in conjunction with optical fibres
- 6 Remote sensing is possible when used in conjunction with optical fibres

**TABLE 1.2**

**TECHNOLOGICAL APPLICATIONS ENHANCED BY USE OF OPTICAL SENSORS**

- 1 Anti burglar alarm systems
- 2 Intra board communication between various IC's in the motherboard of a PC
- 3 Various kinds of level sensors in automobiles and aircraft's
- 4 Defence applications (for e g SMART bombs that continuously sense the height above the ground and detonate at a specified height)
- 5 In feedback loop and control system applications
- 6 Fire and smoke alarm systems
- 7 In automated production to sense position thickness and to count the number of finished products on the conveyor belt
8. To sense rotation in aerospace and military applications

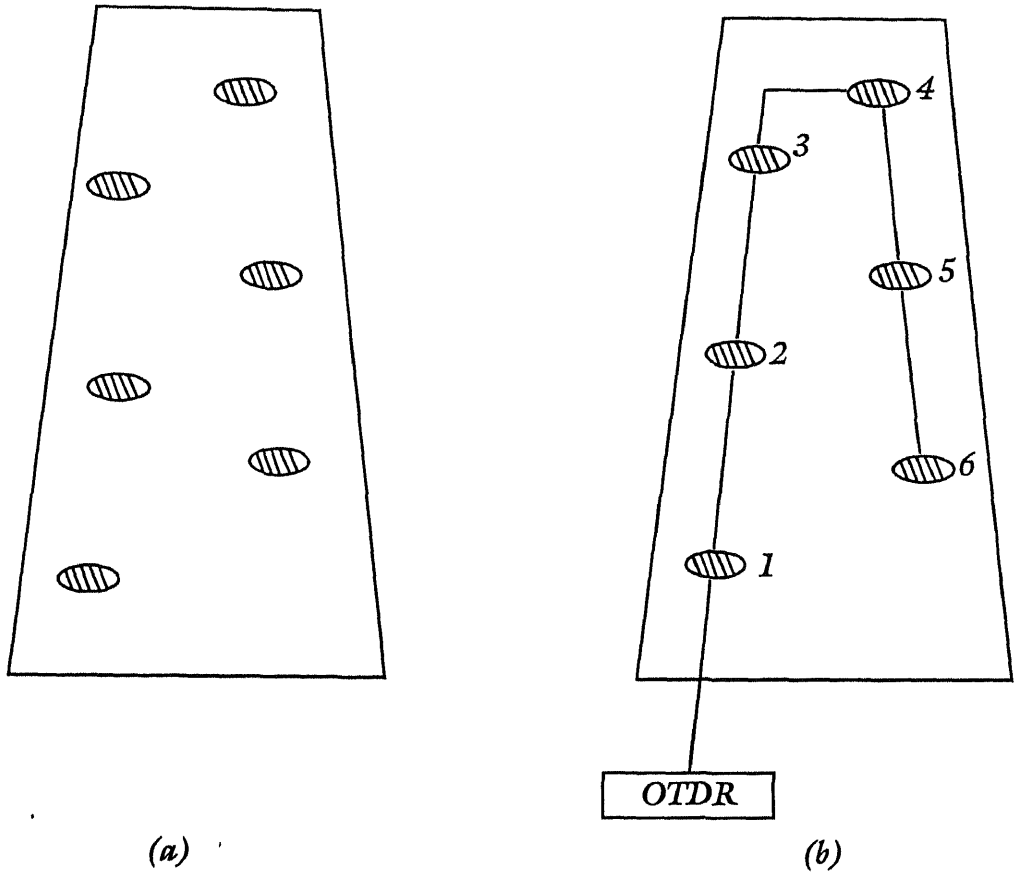


**Fig. 1.1** (a) Air Craft wing with 6 strain gauges distributed over its cross - section  
 (b) Connection of fiber optic strain sensors in wing to OTDR (optical time domain refractometer) using time multiplexing

## CHAPTER 2

### OPTICAL SENSORS

In this chapter we take a close look at optical sensors including their advantages and their classification into various categories. The package design and the approach followed in selecting our low cost optical sensor have also been touched upon. The major issues associated with the design have also been highlighted.

#### 2.1 Types of Optical Sensors

Broadly, optical sensors may be classified under the following three categories

- (a). **Free Space Optical Sensor.** In this sensor the light beam, which interacts with the sensing head, propagates in air / free space
- (b). **Optical Fibre Sensor** In this type of sensor, fibres are used to convey light from the source to the sensor head or the sensing variable acts on the fibre changing the properties of the fibre. The fibre can be sensitised to a large number of measurands like temperature, strain etc and several varieties of optical fibre sensors are available commercially
- (c). **Integrated Fibre Optic Sensors.** These are mostly integrated versions of the fibre optic sensors. They are deployed when small size (mm - micron) and high sensitivities are required, they may be more expensive than the free space optical sensors & the fibre optic sensors [1]

Optical sensors can also be classified on the variety of different mechanisms to turn a change in the measurand into a change in the optical power output of the guided wave optical circuit, which is then sent to a photodetector and processed automatically [2]. The various types of optical sensors may thus be classified as under

- (a). **Intensity Modulated Sensors** The measurand directly changes the intensity of an optical beam transmitted through the sensor. Shown in fig 2.1 is one such sensor where the intensity of

liquid.

**(b). Phase Modulated (Interferometric) Sensors.** In this type of sensor, the measurand causes a phase shift in the incident beam of light or a change in the polarisation of the incident beam that is interfered / compared with a reference beam. Then the shift in phase /polarisation is converted to the variation in output intensity of the optical circuit. Aschematic of this type of sensor is as shown in fig 2.2

## 2.2 Package Design for an Optical Sensor

One of the technical problems that have to be solved for manufacturing and deploying an optical sensor is that of sensor packaging. In all types of sensor designs, packaging is an important issue, but in non-optical cases it is comparatively less significant. The major roles of a package of an optical sensor as already explained in chapter 1 are alignment, thermal stability, shielding from stray radiation's and proper spacing between the various components. In this thesis we have considered the package design for a simple low-cost optical sensor. The requirement of it being low cost meant that the design of the optical sensor should have only a few components. The optical sensor would comprise of the basic components of a source, a detector, a physical variable and a device to keep it in. We selected liquid level measurement to analyse the packaging of a source and detector as liquid level is a physical variable that could be incorporated in our analysis of package design at no additional cost and also for the reason that few automobile & aeronautical concerns had shown an interest in the feasibility of an optical sensor for liquid level measurement. A laser diode or an LED or a fibre illuminator (tips of fibre bundle) may be used as a source in our sensor. The receiving device may either be a PIN photodiode (for in situ measurement) or an optical fibre or fibre bundle for transmitting the signal to a remote distance.

The intensity modulated optical sensors are the simplest and most widely used in the field of optical sensors [3]. Thus for the analysis of our package design, we chose an intensity modulated optical sensor. Starting from a simple design, we kept on modifying the package design to take into account various intricacies that this simple design projected.

The first issue that we had to decide on was the shape of the package & the package design that we have considered is housed in a hollow cylindrical package. Then while deciding on the design for a simple intensity modulated liquid level sensor, we had the option to either go in for a reflective type of sensor or for a refractive type of sensor and we decided to do an analysis of both these types of sensors using geometric optic considerations, and then select a feasible design.

Having decided on the shape of the package and the type of optical sensor to be used, we had to select the type of source to be used (i.e. LED, Laser Diode or fibre illuminator). This selection was done based on the divergence angle of the source. Thus, based on the tentative dimensions of the package, we developed guidelines for parameter selection for the type of source and also evolved a relationship between the under mentioned variables:

- (a) Beam spot size
- (b) Beam divergence angle
- (c) Height & radius of base of cylindrical package
- (d) Detector size
- (e) Surface tension, density, contact angle & refractive index

Once the type of source was decided upon, a fresh analysis was carried out using wave propagation approach. The radius of curvature of the liquid surface was expressed in terms of other known parameters of the package and was taken into account while carrying out the wave propagation analysis.

Such an analysis was carried out for both the reflective and refractive type of optical sensors and two configurations of each type were considered. Subsequently a comparative analysis of these results was carried out and sensor configuration no 3 was selected as it appeared to be a feasible option. In this sensor, as shown in fig 2.3, both the source and the detector are on top of the tube containing the liquid.

The offset, which exists between the source and detector in reflective type of sensors, was also considered and incorporated in the analysis of these sensor configurations

Also, a prototype design for an "annular ring shaped detector" based optic sensor was proposed, which eliminated the lateral offset between source and detector. The analysis of a sensor with an annular ring shaped detector was also carried out

## REFERENCES

- [1] S S Sekhon, M Tech thesis on "Design of Reflective Fibre Optic Sensors for Displacement Measurement", Laser Technology Programme, IIT Kanpur, 1998
- [2] A.B Buckman, "Guided Wave Photonics", Saunders College Publishing, New York, 1996. Chapter 9
- [3] B P Pal (Ed), "Fundamentals of Fibre Optics in Telecommunications and Sensor systems" Wiley Eastern, New Delhi, 1992, Chapter 22

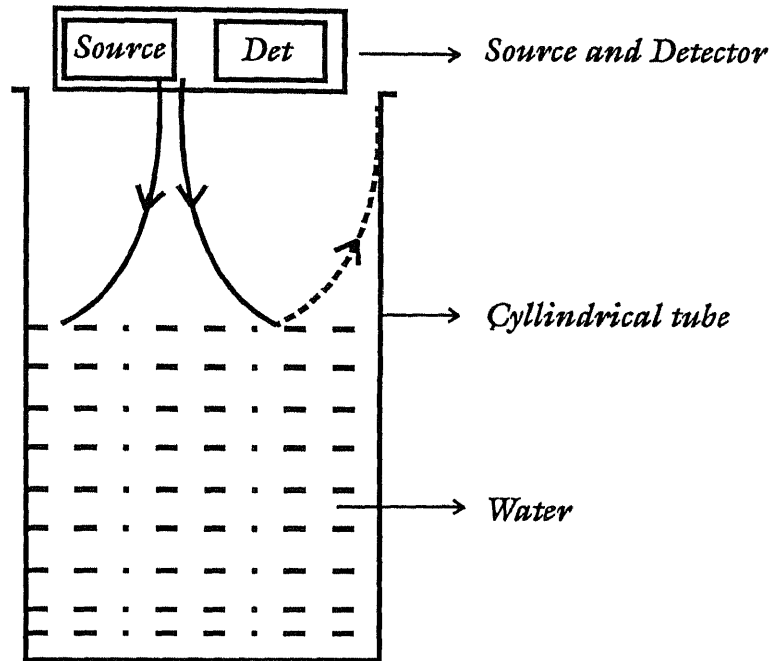


*Fig. 2.1 A Simple intensity modulated optical sensor*

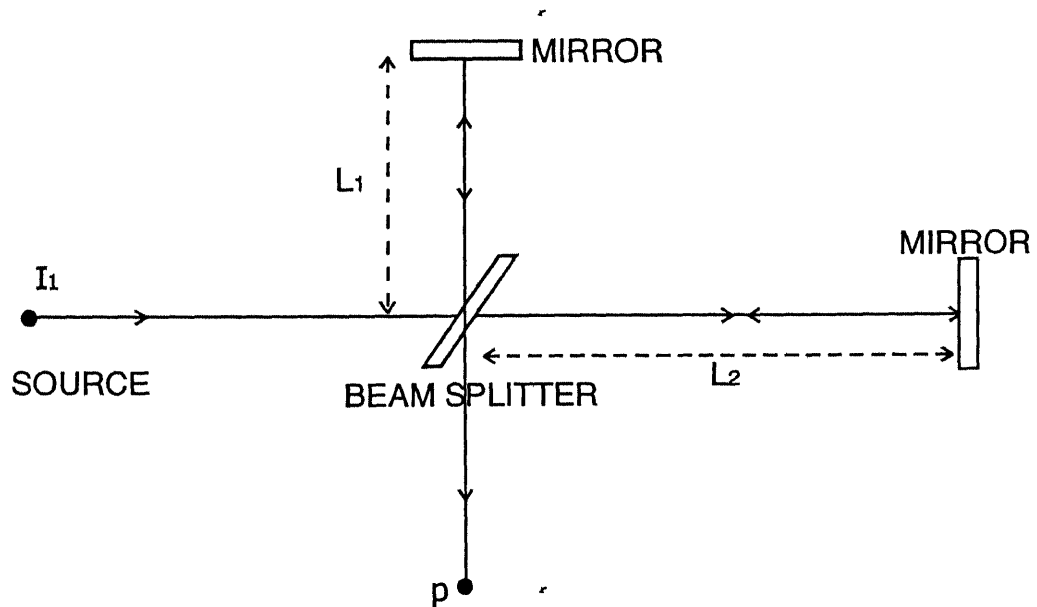


*Fig. 2.2 A Michelson Interferometer realized with conventional bulk optic components.*

## CHAPTER 3

### LIQUID LEVEL SENSORS

We selected liquid level measurement to analyse the packaging of a source and detector as liquid level is a physical variable that can be measured with no additional transducer. The liquid surface and /or the bulk of the liquid interacted with the light beam changing its intensity as the height of the column varied. Also we did not find such simple liquid level sensors reported in literature.

#### 3.1 Various Types of Liquid Level Sensors.

Liquid level is an important variable that is measured in aircraft's process industries and many other areas using various kinds of sensor. These technologies are based on floats, capacitive sensors, ultrasound and nuclear radiation techniques [1]. These technologies are

(a). **Float.** As shown in Fig (3 1), a plastic air filled ball is hinged to the top of the vessel containing the liquid. the ball floats on top of the liquid surface. A pointer is attached at the other end of the device holding the ball. The pointer moves along a calibrated scale indicating the liquid level. When the liquid level is low the ball floats on top of the liquid but at a low level as shown in Fig 3 1 (a), and the pointer indicates a low level. As the liquid level increases, the ball rises and the pointer attached to the other end of the rod moves towards the " full "(maximum) level indicator. This type of liquid level sensor is easy to make and it is widely used. It is a low cost device but its accuracy is not high.

(b). **Capacitive Type** A schematic diagram of this type of sensor is shown in Fig (3 2). A cylinder is introduced in the middle of a tank containing the liquid. If ' d ' is the separation between the positively and negatively charged plates, ' A ' is the surface area and '  $\epsilon$  ' is the permittivity of the liquid, then the capacitance 'C' is given by  $C = \epsilon A / d$ . A and d being constants, C is directly proportional to  $\epsilon$  and the value of  $\epsilon$  can be mapped on to the liquid level. Thus 'C' is proportional to liquid level and can accordingly be calibrated.

This type of sensor is used in aeronautical and automobile industry. Its main advantage is that this technology is widely accepted and it can be manufactured easily. However, the change in capacitance due to the change in the value of  $\epsilon$  is usually small and thus we are only able to monitor the liquid level using complex electronics if we want accurate results. Also, the presence of a number of wires to and from the sensor, are a potential source of fire hazard, especially in confined spaces like aircraft's. Due to this reason the measurement of capacitance also changes.

(c). **Ultrasound Sensors.** As shown in Fig (3.3) ultrasound waves are emitted from a source strike the surface of the liquid and get reflected back to the sensor where they are detected. The time interval between emission and receipt of the signal is directly dependent on the distance between the ultrasound source and the surface of the liquid. This time interval is mapped on to the liquid level and measurement is done. This type of sensor is widely used in marine applications by ships to know the depth of water at a particular spot and is accurate.

(d). **Optical Liquid Level Sensor** The optical liquid level sensors are mainly intensity modulated sensors. A number of optical sensors have been reported. Most of these are fibre optic sensors based on differential absorption [2], bending induced mode coupling [3], [4] and index dependent total internal reflection [5]. These sensors are suitable for measurement of discrete liquid levels. Continuous sensors have been designed on the principles of optical radar [6] and index induced waveguide coupling at a liquid surface [7]. These can be classified under the following categories.

As shown in Fig (3.4), in this type of sensor, fibres are used to convey light from the source to the sensor head. After being reflected from the liquid surface, the light is conveyed back to the detector through a fibre. These types of sensors are good and can be used to access inaccessible areas.

### 3.2 A Simple Optic Liquid Level Sensor for a Case Study in Package Design

For a case study in package design we chose a free space optical sensor that can measure the liquid level continuously. We put the liquid whose level is to be measured in a cylindrical container and bring an optical source and a photodetector in the proximity such that the intensity of the light falling on the photodetector is changed by a refraction through the liquid column or by a reflection from the liquid surface. In Fig (3.5), we show one possible configuration with source and detector are placed on top and bottom respectively of the tube containing the liquid. This type of level sensor is easy to implement. Due to its inherently dielectric construction, there is no risk of arcing and thus this sensor can be used for measurements in a hazardous environment. Thus this sensor overcomes the disadvantages of the capacitance type of sensor. Also, this type of sensor can be used to measure the curvature of the liquid surface.

There are four different ways in which a source and a detector can be arranged, to design a this type of simple low cost optical liquid level sensor. The first arrangement is shown in Fig (3.5). In the second arrangement, the detector is kept at the top of the tube containing the liquid and the source is at the bottom of the tube. This topology will hereafter be referred to as "Sensor Configuration No 2" and the same is shown in Fig (3.6). In the third arrangement, both the source and detector are kept at the top of the tube containing the liquid. This topology will hereafter be referred to as "Sensor Configuration No 3" and the same is shown in Fig (3.7). In the last arrangement, both the source and detector are kept at the bottom of the tube. This topology will now be referred to as "Sensor Configuration No 4" and the same is shown in Fig (3.8).

Of these four topologies listed above, the first two are examples of transmissive type and are intrinsic type of intensity modulated sensors. The first two, that is Configuration no's 3 and 4, are transmissive type and are intrinsic type of intensity modulated sensors.

Even for these simple structures we need to select the type of source to be used, the type of the detector required, the tube height and diameter and the separation between the source and detector to

package the optical sensor. In addition to these package design parameters, it is also necessary to select the range of optical power incident from the source, the wavelength at which the source is required to operate and the minimum spot size of the gaussian beam at that wavelength. We studied the selection of parameters using both geometric optic analysis and wave propagation considerations. The geometric optic analysis provided us with guidelines for parameter selection and helped in the selection of the type of source to be used for the optical sensor. However, a detailed analysis of these simple structures was possible using wave propagation considerations.

## REFERENCES

- 1 S S Sekhon, M Tech thesis on " Design of Reflective Fibre Optic Sensors for Displacement Measurement", Department of Laser Technology, I I T Kanpur, 1998
- 2 J P Dakin and M G Holliday, "A liquid level sensor based on OH or CH absorption monitoring ", Proc First Int Conf Optical Fibre Sensors, Vol 221, pp 91 - 95, April 1983
- 3 AL Harman, " Optical Fibber Refractometer using attenuation of cladding modes ", Proc First Int Conf Optical Fibre Sensors, Vol 221, pp 104 - 108, April 1983
- 4 K Spenner et al, " Experimental Investigations on fibre optic liquid level sensors and refractometers ", Proc First Int Conf Optical Fibre Sensors, Vol 221, pp 96 - 99, April 1983
- 5 D A Jackson, "High Precision remote liquid level measurement using a combination of optical radar and optical fibres ", Proc First Int Conf Optical Fibre Sensors, Vol 221, pp 200 - 203, April 1983
- 6 G Bitta and L Ippolito et al, " An optical fibre based technique for continuous liquid level sensing ", IEEE Trans on Instrumentation and Measurement, Vol 44, No 3, pp 686 - 689, 1995
- 7 A Yarrv, " Optical Electromcs ", Holt Rinehart and Winston, New York, Chapter 2, p 32, 1985

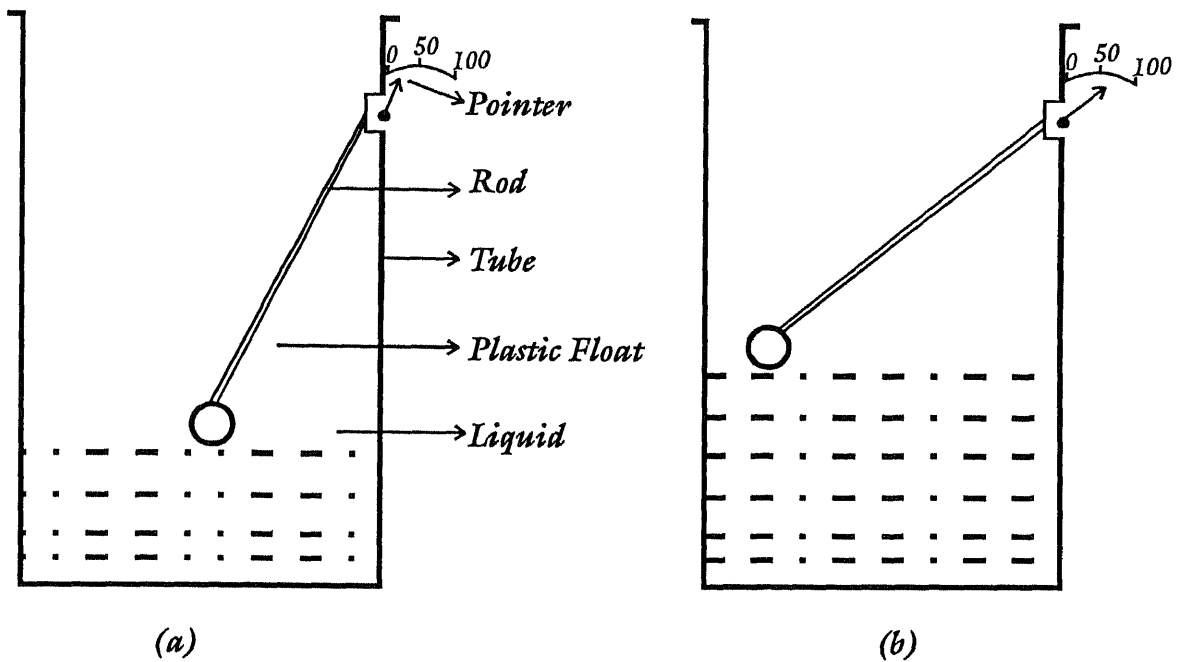


Fig. 3.1 (a) Float indicating less level of liquid  
(b) Float indicating liquid level nearly at half way mark

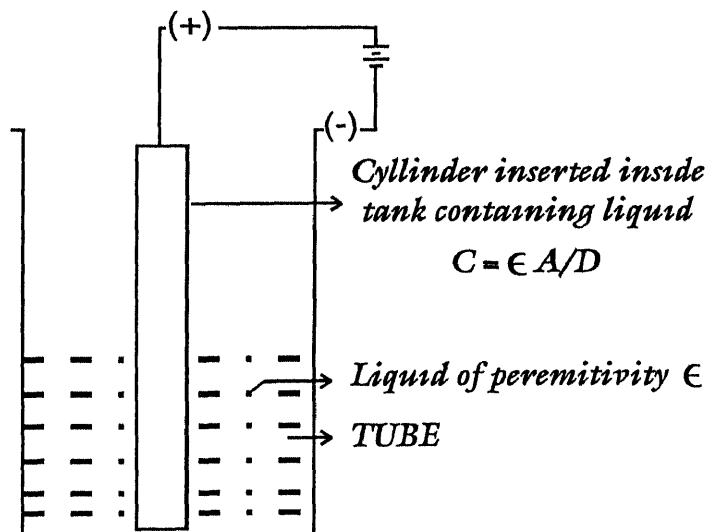
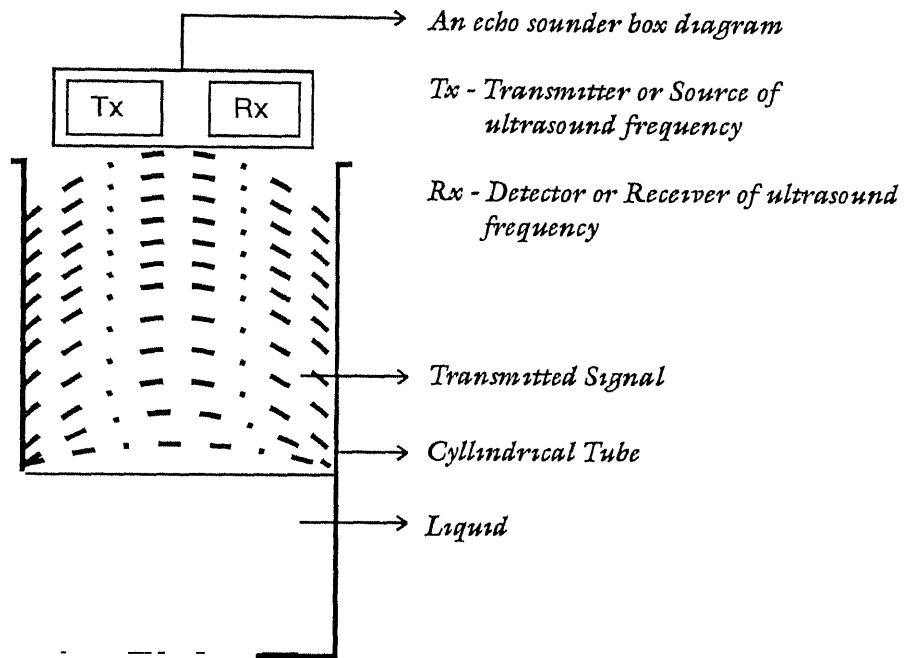
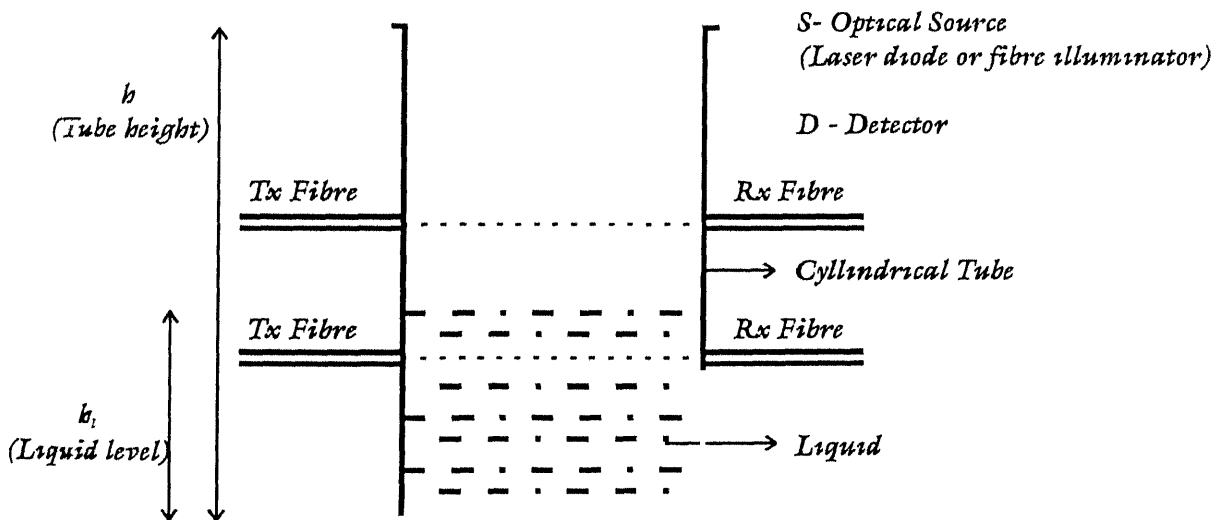


Fig. 3.2 Capacitive type of liquid level sensor



*Fig. 3.3 An Ultrasound Liquid Level Sensor*



*Fig. 3.4 A Fibre Optic Liquid Level Sensor*

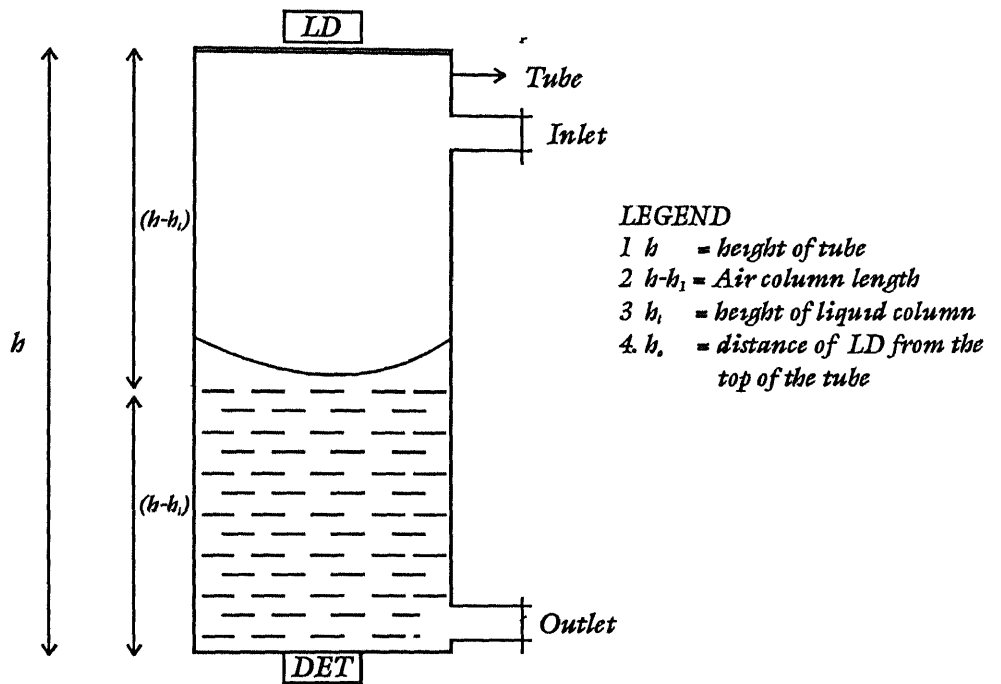


Fig. 3.5 Sensor configuration No. 1

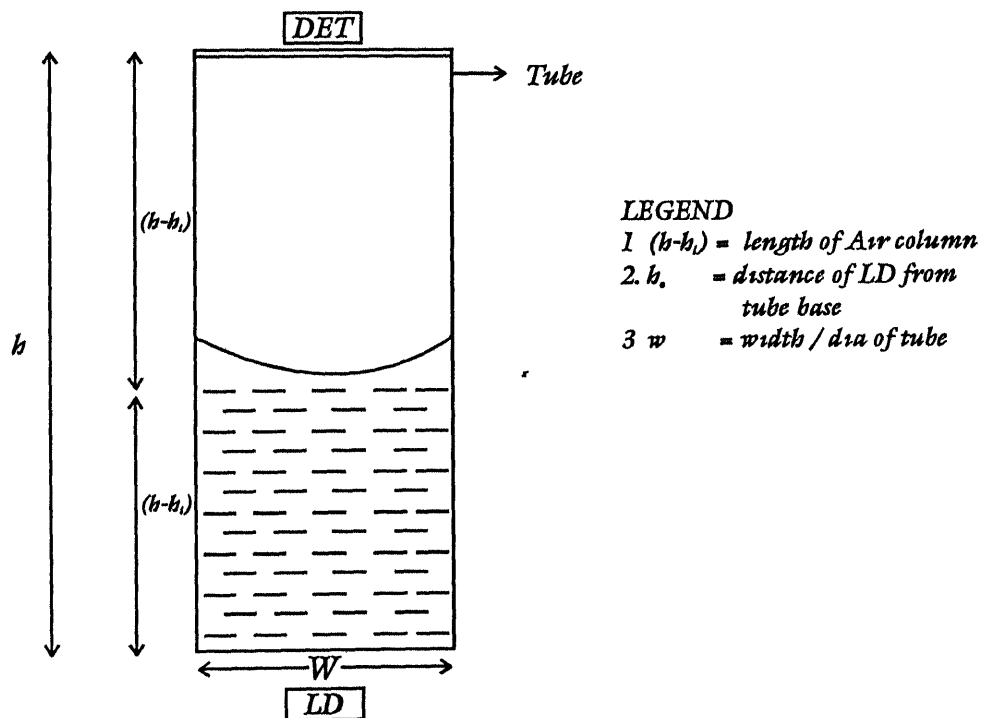


Fig. 3.6 Sensor configuration No. 2

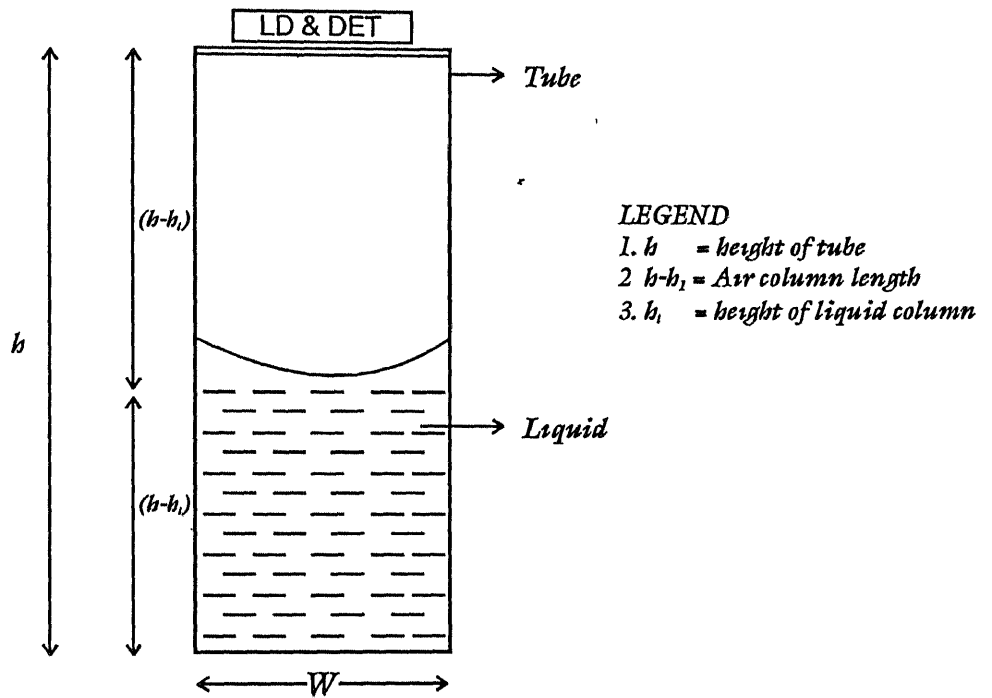


Fig. 3.7 Sensor configuration No. 3

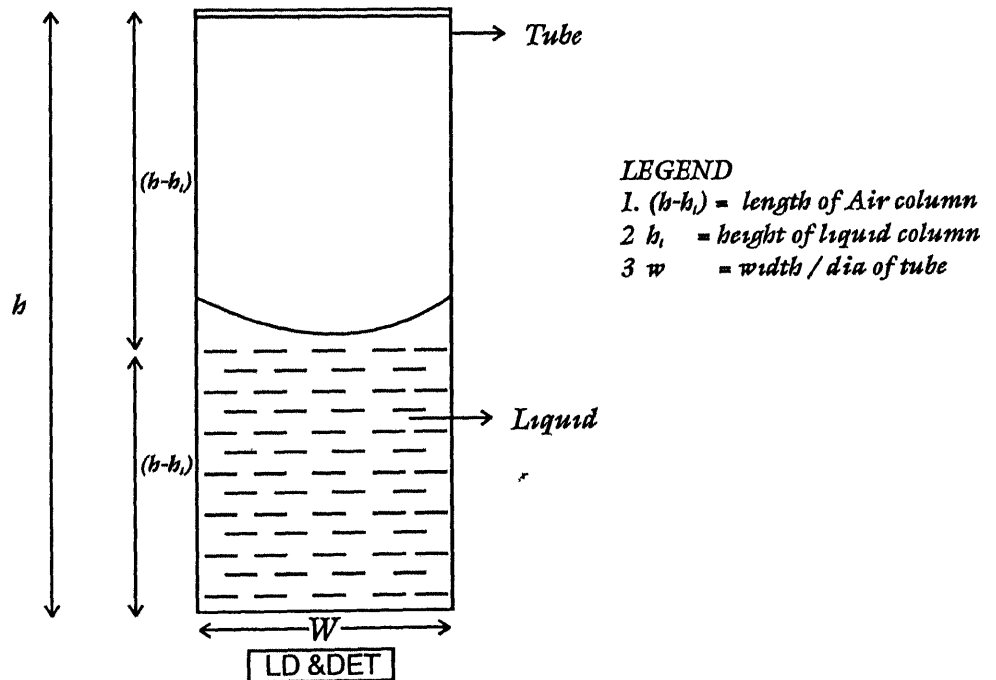


Fig. 3.8 Sensor configuration No. 4

## CHAPTER 4

### GEOMETRIC OPTICS APPROACH FOR STUDY OF OPTICAL

#### LIQUID LEVEL SENSOR ARCHITECTURE

Geometric optics or ray optics is a simple way of describing the behaviour of light. We first study the optical liquid level sensor architectures using ray optics to derive design guidelines. The four possible configurations of our low cost liquid level sensor are as shown in fig 4.1. Fig 4.1(a) and (b) pertain to the transmissive type of optical sensor, in which the source or detector is at the top of the tube respectively. One important consideration in the design was that there should be no multiple ray paths from the source to the photo detector owing to the reflection of rays from the sidewalls of the tube. If multiple rays reached the photo detector, then it would be difficult for the photo detector to discern which ray is incident upon it directly and which ray arrives after being reflected from the sidewalls of the tube. There is also a possibility that the ray which is directly incident on the photo detector and a ray which reaches photo detector after being reflected from the side walls, arrive at the photo detector at the same time. In such an instance both these rays will add up and the effect of any one beam will not be seen.

#### **4.1 Data Used For Generation of Results**

Based on geometric optics we will analyse all the four configurations and establish a relationship between the various physical parameters of each sensor. An idea about the beam divergence angle of a source (LED, Laser Diode or Fibre illuminator) can be obtained from the geometric optic analysis. We thus try to calculate the maximum value of the half divergence angle, in each of the four topologies discussed in chapter 3, in order to get an idea of the acceptable limit of the beam divergence angle and thus decide upon the type of source to be used for our optical sensor.

Having established a relationship between the various physical parameters of each sensor and the beam divergence angle of a source in all the four configurations, programmes are written to evaluate its value.

The programmes can be run by any user by inputting various values of design parameters such as tube height  $h$ , tube width  $w$  and refractive index of liquid  $n_2$ . The values of all these parameters had to be selected to suit the specifications of our low cost optical sensor.

There is a requirement of an optical window to be put on the base of the tube for transmissive type of sensors (sensor configuration No's 1 and 2) Optical windows come in specified sizes and due to the complexity in their fabrication process, their cost increases as their size becomes larger For our low cost optical sensor, the optical window should be large enough to accommodate the source and detector Thus an optical window with a diameter of approximately an inch (25.4 mm) would suffice for our purpose Keeping a margin of 1.2 mm on either side of the diameter to allow for fixing the optical window to the walls of the tube, at the base of the tube we are left with an optical window with a diameter of 23 mm

The tube in which the liquid is kept though should not be so long that it becomes unwieldy to handle, yet it should be long enough to allow proper measurement of the liquid level by our optical sensor In view of this, a tube of length = 10 cm (100 mm) would meet the requirement Moreover, the range over which the sensor should be able to function should be starting from 5 mm from the base of the tube to 10 mm short of the top of tube In view of this, a tube of length = 11.5 cm (115 mm) would meet the requirement as this would allow measurement to be done over a range of 10 cm (100 mm) Moreover, HAL private communications limited had also projected the requirement that the liquid measurement should be possible over a length of 10 cm The liquid selected for the purpose of our analysis is water and the refractive index of 1.33 has been accordingly selected The values of various parameters thus chosen to find the value of 'half beam divergence angle', for various values of liquid level are as listed below

(a) Diameter of tube	23 mm
(b) Height of tube	115 mm
(c) Refractive index of liquid	1.33

#### 4.2 Beam Divergence Angle

An idea about the beam divergence angle of a source (LED, Laser Diode or Fibre illuminator), can be obtained from the geometric optic analysis We thus try to calculate the maximum value of the half

divergence angle, in each of the four topologies discussed in chapter 3, in order to get an idea of the acceptable limit of the beam divergence angle and thus decide upon the type of source to be used for our optical sensor

In the course of this analysis we make the following assumptions -

- (a) The source and detector are placed at the centre of the tube containing liquid in order to ensure that the half divergence angles on either side of the centre of tube are same and is equal to half of that of the actual divergence angle of the source
- (b) Reflectivity of the surface is 100 %
- (c) The beam emitted by the point source is lambertian in nature, so as to be able to use the value of the divergence angle to calculate the intensity received by detector
- (d) The reflecting surface is much larger than the wavelength of the light.
- (e) Diameter of the source and detector is much smaller than the distance between the source/detector and reflecting surface

### 4.3 Half Divergence Angle Relationships and Results

In order to ensure that no sidewall reflections take place, the source and detector were placed in the centre of the tube. Also, assuming that the most divergent ray emitted by the source would land at the edge of the base of the tube, the half divergence angle was calculated. Given in the subsequent paragraphs, is the analysis of each of the four possible architectures of our liquid level sensor

**4.3.1 Analysis of Sensor Configuration No 1:** In this configuration as shown in fig 4.1, the source is at the top of the tube of height 'h' filled upto a height 'h<sub>1</sub>', with a liquid of refractive index n<sub>2</sub>. The equation relating the value of half divergence angle (hereafter referred to as HDA)  $\theta$  with the other parameters is

$$\theta = \sin^{-1} \left\{ (n_2/n_1) (w - b \tan \theta) / (2 h_1 \sqrt{1 + \left( \frac{w - b \tan \theta}{2 h_1} \right)^2} \right\} \quad (4.1)$$

where,  $n_1$  = refractive index of air =1,  $n_2$  = refractive index of liquid.  $h_1$  = height of liquid column from base of tube . $b = h_o + h - h_1$  ,  $h_o$  = distance of laser diode from top of tube , $h$  =height of tube , $w$ = width of tube

Rearranging equation 4 1 and rewriting we get a transcendental equation in  $\tan \theta$  as under

$$\tan^2 \theta (b^2 (1-a^2)) + \tan^3 \theta (2wb(a^2-1)) + \tan^2 \theta (c^2 + w^2 - a^2(w^2 + b^2)) + \tan \theta (2wb a^2) - a^2 w^2 = 0 \quad (4.2)$$

where  $a = n_2/n_1$  and  $c = 2h_1$

Evaluating equation (4.2) using Newton Raphson method [3] , we get the value of  $\theta$  for various combinations of the values of  $h_o$  and  $h_1$  , such that no side wall reflections take place , and these are listed in Table 4.1 These values of ' $\theta$ ' were obtained for the test data before The liquid level ( $h_1$ ) was varied from 0 mm, 10 mm, 50 mm , 100 mm and 115 mm and the offset or distance of source from the top of the tube ( $h_o$ ) was varied from 0 mm to 5 mm in steps of 1 mm This same test data has been used during the analysis of the other optical sensor topologies, which are explained in this section.

**4.3.2 Analysis of Sensor Configuration No 2 :** In this configuration as shown in fig 4.2 , the detector is at the top of the tube of height 'h' filled upto a height ' $h_1$ ' ,with a liquid of refractive index  $n_2$  The desired transcendental equation relating  $\theta$  with other physical parameters is given by

$$\tan^2 \theta (p^2 (a^2 - 1) + a^4) - p^2 = 0 \quad (4.3)$$

where,

$$p^2 = (w^2 k_5 + k_2 b^4 + k_3 b^2 + k_4 \sqrt{k_5} b^2 - 4wbh_o k_5 - 4wbh_1 \sqrt{k_5}) (1/(k_5 k_6))$$

where  $a = n_2/n_1$  , and the constants  $k_1, k_2, k_3, k_4, k_5, k_6$  are mathematical expressions relating the variables and constants pertaining to the dimensions of the tube and to the liquid ,for ease of computation Solving equation 4.3 by Newton Raphson method and using the same test data as was used for the

analysis of optical sensor configuration No 1, we get the value of  $\theta$  for various combinations of the values of  $h_o$  and  $h_1$ , such that no side wall reflections take place, and these are listed at Table 4 2

**4.3.3 Analysis of Sensor Configuration No 3.** In this configuration as shown in fig 4 3, both the source and detector are at the top of the tube of height 'h' filled upto a height ' $h_1$ ', with a liquid of refractive index  $n_2$ . The desired transcendental equation relating  $\theta$  with other physical parameters is given by

$$k_3 \tan^4 \theta + k_4 \tan^2 \theta + k_5 \sqrt{k_7} \tan \theta - k_6 = 0 \quad (4.4)$$

where the constants  $k_1, k_2, k_3, k_4, k_5, k_6$  and  $k_7$  are mathematical expressions relating the variables and constants pertaining to the dimensions of the tube and to the liquid, for ease of computation and the symbols  $h_o$  and  $n_1$  have meaning as explained in section 4 2 (a)

Solving equation 4 4 by Newton Raphson method and using the same test data as was used for the analysis of optical sensor configuration No 1, we get the value of  $\theta$  for various combinations of the values of  $h_o$  and  $h_1$ , such that no side wall reflections take place, and the same are listed at Table 4 3

**4.3.4 Analysis of Sensor Configuration No 4.** In this configuration as shown in fig 4 4, both the source and detector are at the base of the tube of height 'h' filled upto a height ' $h_1$ ', with a liquid of refractive index  $n_2$ . The desired transcendental equation relating  $\theta$  with other physical parameters is given by

$$k_3 \tan^2 \theta (k_1 - 4 h_o^2) - 8 h_o h_1 \sqrt{k_3} \tan^2 \theta - 4 h_1^2 \tan^2 \theta + 4 w h_o k_3 \tan \theta + 4 w h_1 \sqrt{k_3} \tan \theta - k_3 w^2 = 0 \quad (4.5)$$

where the constants  $k_1, k_2$  and  $k_3$  are mathematical expressions relating the variables and constants pertaining to the dimensions of the tube and to the liquid, for ease of computation and the symbols  $h_o$  and  $n_1$  have meaning as explained in section 4 2(a)

Solving equation 4.5 by 'Newton Raphson' method and using the same test data as was used for the analysis of optical sensor configuration No 1, we get the value of  $\theta$  for various combinations of the values of  $h_o$  and  $h_l$ , such that no side wall reflections take place, and the same are listed at Table 4.4

#### 4.4 Comparative Analysis

A comparative analysis of the results obtained from all the 4 topologies is tabulated as under. For each optical sensor configuration, for a particular combination of the offset ( $h_o$ ) and the liquid level ( $h_l$ ), there is a smallest value of half maximum divergence angle (HMDA) that is  $\theta_{small}$  hereafter abbreviated as  $\theta_s$ , and a largest value of HMDA that is  $\theta_{large}$  hereafter abbreviated as  $\theta_l$ . The values of  $\theta_s$  and  $\theta_l$  (in degrees) for each of the four architectures, for the test data listed in section 4.1(a) of this chapter, is listed at table 4.5

It was observed that for all four cases analysed,  $\theta_l$  always occurred when the offset ( $h_o$ ) is the smallest of the 5 values over which it is varied and the liquid level ( $h_l$ ) is the largest of the values over which it is varied, that is from '0' to 'h'. Also,  $\theta_s$  always occurred when ' $h_o$ ' is the largest of the 5 values over which it is varied and ' $h_l$ ' is the largest of the values over which it is varied.

#### 4.5 Parameter Selection and Type of Source

The reasons for selecting the values of the tube length, tube diameter and refractive index of the liquid have already been explained in section 4.1 of this chapter and the values of these three parameters are 115mm, 23mm and 1.33 respectively. The HDA of a light cone emitted by the source was calculated for a tube having a height = 115 mm and radius = 11.5 mm, and the results are tabulated as per table's 4.1 - 4.4. On analysis of the results it was found that the laser diode would be a suitable choice for the source as its divergence angle is in 'milli radians' and it meets the requirements of the values of HMDA calculated for the four topologies being considered for an optical sensor.

An LED can be used as a source , but a source generating a coherent and directional beam of light would , be better in performance to an LED and as such the laser diode was found to be an appropriate choice for the source

The relationship developed between the HMDA ' $\theta$ ' , the height of the tube 'h' ,the tube diameter 'w' and the height of liquid level ' $h_l$ ' as listed in equations 4.2 to 4.5 , can also be used for parameter selection by the package designer / manufacturer of the optical sensor as any one of the parameters can be expressed in terms of the other parameters

An idea about the shape of the vessel in which the liquid should be kept in order to minimise sidewall reflections ,can also be made For example, for sensor configuration No 3 ( in which both the laser diode and detector are on top of the tube ) , a tube whose diameter increases gradually on going from top towards the bottom , would be ideally suited to minimise the occurrence of side wall reflections However , a more detailed analysis about this aspect could be done subsequently

#### 4.6 Summary

Using the ' Geometric Optics Approach ' to carry out the analysis of the four possible topologies of our low cost optical sensor ,it was found that the laser diode would be a suitable choice for the source of the low cost optical sensor (LCOS ) A set of values of the tube parameters for our low cost optical sensor , have also been selected A feasible shape of the tube in which the liquid is to be kept has also been proposed However , in order to do a more detailed analysis and obtain further information about various design parameters , the wave propagation analysis was carried out and the same is available in the next chapter of this thesis

## REFERENCES

- 1 J.R.Meyer Arendt , "Introduction to Classical and Modern Optics ", Prentice Hall Inc , Eaglewood Cliffs , New Jersey , 1972
- 2 A Ghatak and K Thyagarajan , " Classical Modern Optics ", Tata McGraw Hill Publishing Co Ltd , New Delhi , 1988
- 3 Saul Teukolsky , William Vetterling et al , " Numerical Recipes in C, The Art of Scientific Computing", Cambridge University Press , London
- 4 Matlab User Manual - Student Edition, Mathwork Inc, U.S.A, 1994

**TABLE 4 1**

Values of  $\theta$  (in degrees) for various combinations of the values of  $h_o$  and  $h_1$  for Sensor Configuration No1

$h_o \downarrow h_1$	0 mm	10 mm	50 mm	100 mm	115 mm
0	5 7106	5 8365	6 4021	7 2879	7 6048
1	5 6619	5 7854	6 3406	7 2081	7 5179
2	5 6137	5 7352	6 2803	7 1031	7 4330
3	5 5664	5 6859	6 2211	7 0538	7 3499
4	5 5199	5 6374	6 1630	6 9790	7 2687
5	5 4742	5 5897	6 1060	6 9059	7 1893

**TABLE 4 2**

Values of  $\theta$  (in degrees) for various combinations of the values of  $h_o$  and  $h_1$  for Sensor Configuration No 2

$h_o \downarrow h_1$	0mm	10 mm	50 mm	100 mm	115 mm
0	3 2247	3 3934	4 2923	6 4401	7 5133
1	3 2091	3 3761	4 2648	6 3782	7 4285
2	3 1937	3 3590	4 2376	6 3175	7 3456
3	3 1784	3 3421	4 2108	6 2579	7 2646
4	3 1632	3 3254	4 1843	6 1994	7 1853
5	3 1482	3 3088	4 1582	6 1420	7 0954

**TABLE 4 3**

Values of  $\theta$  ( in degrees ) for various combinations of the values of  $h_o$  and  $h_1$  for Sensor Configuration No 3

$h_o \downarrow h_1 \rightarrow$	0 mm	10 mm	50 mm	100 mm	115 mm
0	0 0249	0 0299	0 0776	1 2541	6 7687
1	0 0245	0 0293	0 0753	1 1218	6 7558
2	0 0241	0 0288	0 0731	1 0085	6 5883
3	0 0237	0 0282	0 0710	0 9110	6 1237
4	0 0233	0 0277	0 0689	0 8264	5 4725
5	0 0229	0 0272	0 670	0 7528	4 8720

**TABLE 4 4**

Values of  $\theta$  ( in degrees ) for various combinations of the values of  $h_o$  and  $h_1$  for Sensor Configuration No 4

$h_o \downarrow h_1 \rightarrow$	0 mm	10 mm	50 mm	100 mm	115 mm
0	5 7106	5 8365	6 4021	7 2878	7 6048
1	5 6617	5 7854	6 3406	7 2082	7 5180
2	5 6136	5 7352	6 2803	7 1300	7 4331
3	5 5663	5 6859	6 2211	7 0540	7 3498
4	5 5198	5 6374	6 1631	6 9990	7 2689
5	5 4741	5 5891	6 1061	6 9060	7 1895

TABLE 4.5

The values of  $\theta_s$  and  $\theta_1$  (in degrees) for each of the four Configurations

	Sensor Configuration No			
	No 1	No 2	No 3	No 4
$\theta_s$ and $\theta_1$	5 4742	3 1482	0 0229	5 4741
$\theta_s$ and $\theta_1$	7 6048	7 5133	6 7687	7 6048

where  $\theta_s$  is the smallest value of half maximum divergence angle (HMDA ), and  $\theta_1$  is the largest value of HMDA

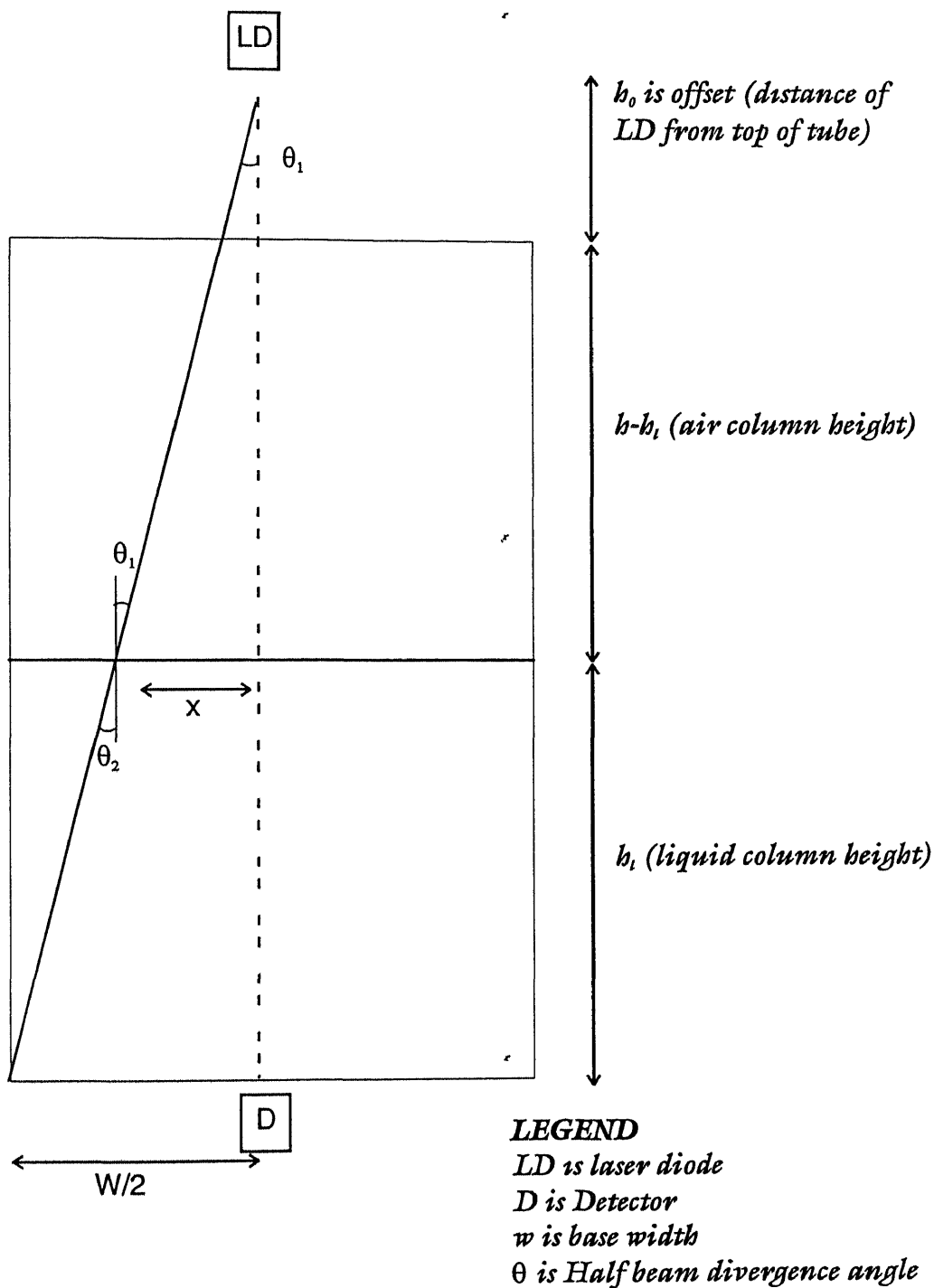
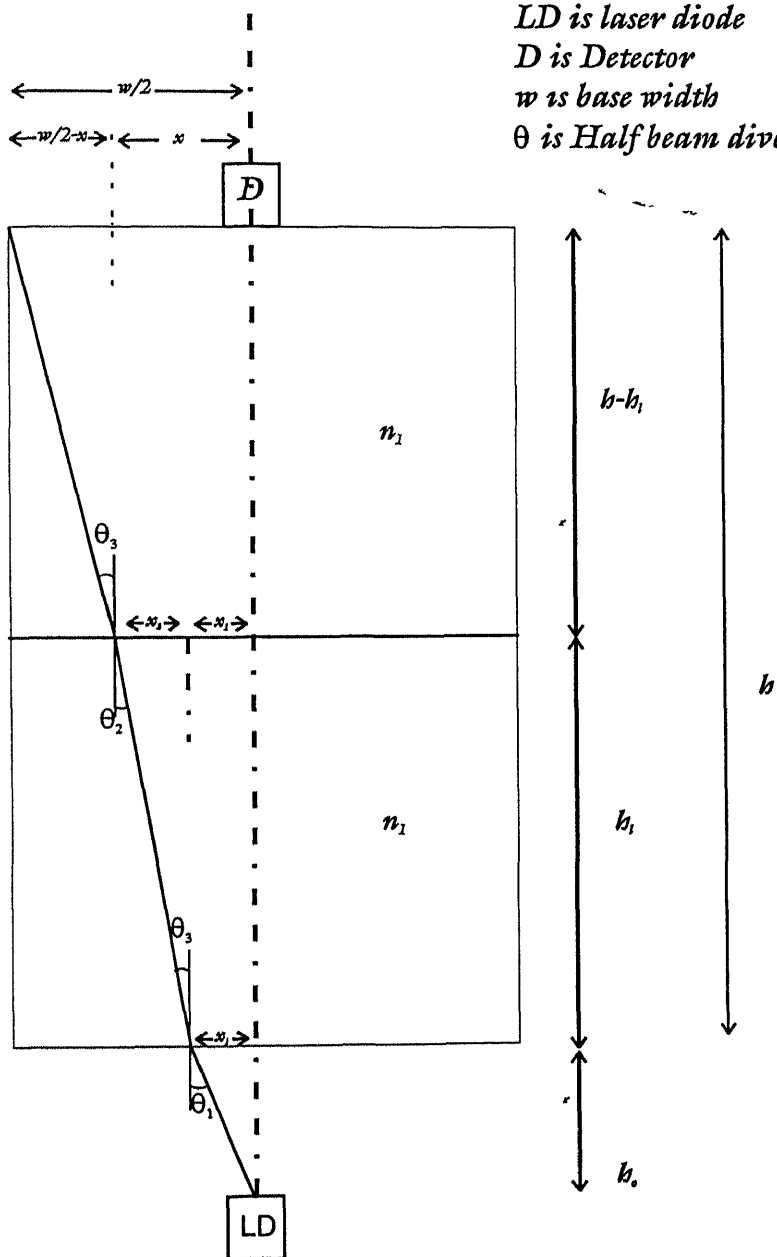


FIG. 4.1 ANALYSIS OF CONFIGURATION NO.1



### LEGEND

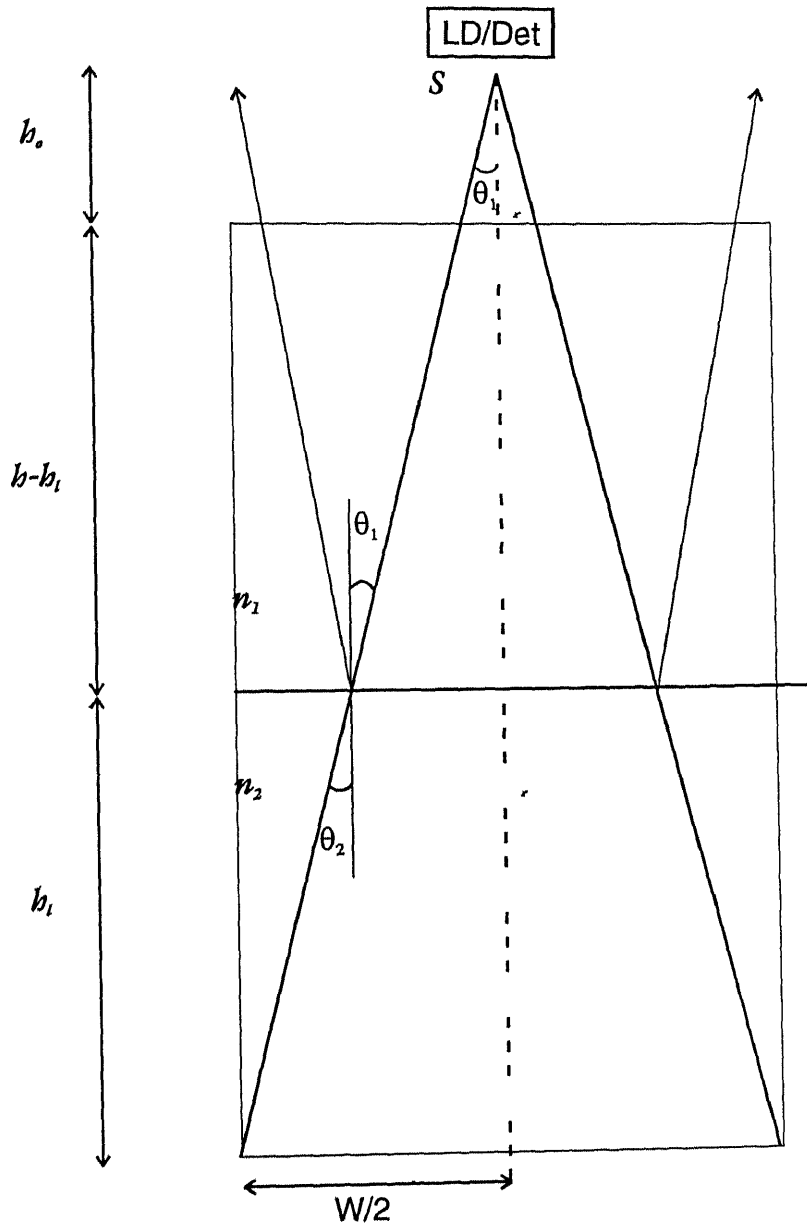
LD is laser diode

D is Detector

$w$  is base width

$\theta$  is Half beam divergence angle

FIG. 4.2 ANALYSIS OF CONFIGURATION NO.2  
(LD AT BOTTOM & DETECTOR AT TOP)



**LEGEND**

*LD is laser diode*

*Det is Detector*

*w is base width*

*$\theta$  is Half beam divergence angle*

**FIG. 4.3 ANALYSIS OF CONFIGURATION NO.3**  
(Both LD and detector placed on top of the tube)

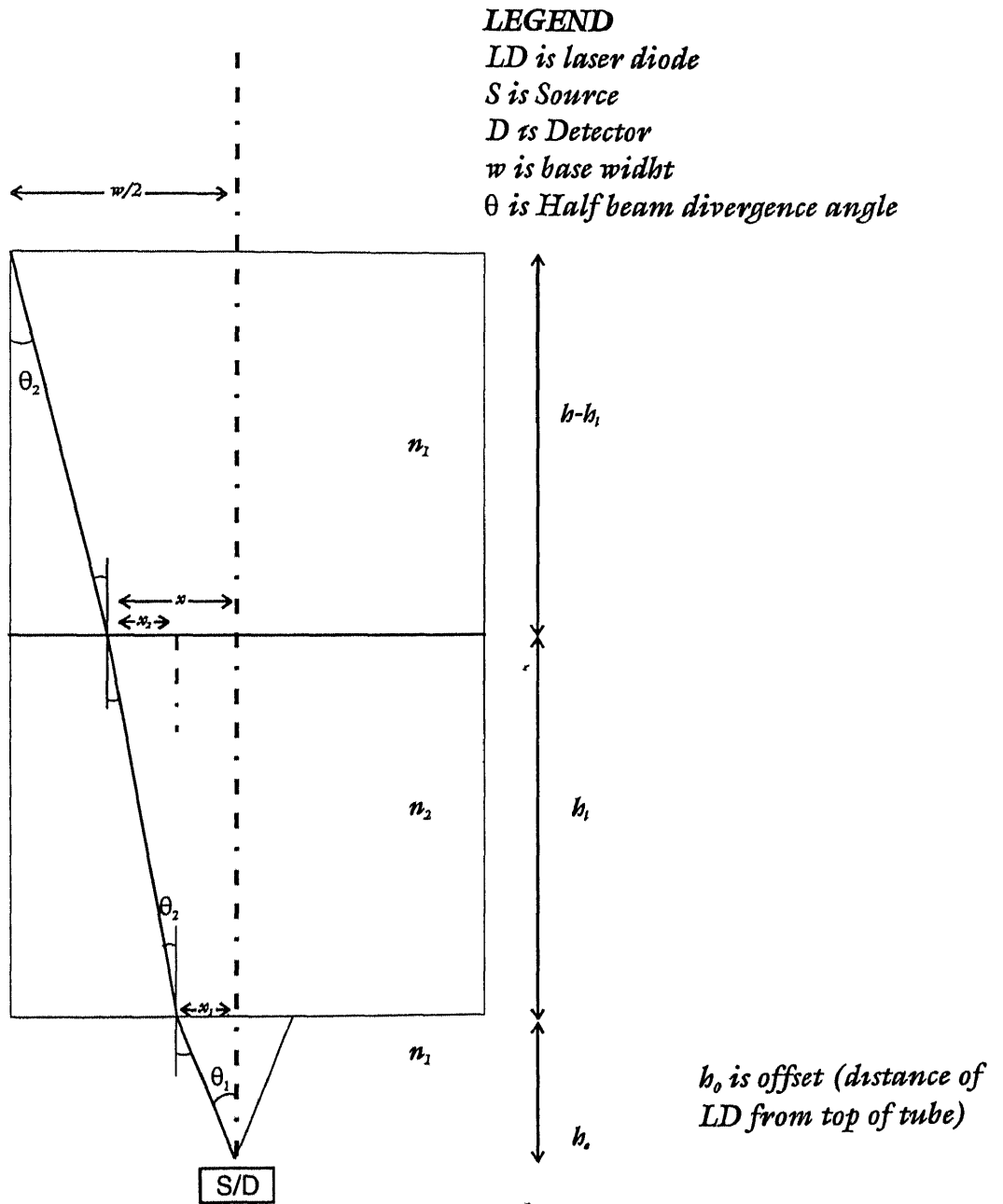


**FIG. 4.4 ANALYSIS OF CONFIGURATION NO.4**  
 (Both LD and Det at base)

**WAVE PROPAGATION ANALYSIS**

To get more insight about the package design of our optical level sensor, the four possible architectures for the level sensor proposed in chapter 3 have been analyzed using the physical optics considerations. While carrying out the analysis, the radius of curvature 'R' of the liquid surface has also been incorporated.

The four possible architectures for an optic liquid level sensor were analyzed and the expression for the final spot size reaching the detector, in all the four cases was derived and the power received at the detector was calculated. It was intended to select one out of these four configurations to fabricate a liquid level sensor and the parameters were chosen accordingly as explained in chapter 4.

**5.1 Shape of Liquid Meniscus**

The shape of the liquid meniscus in any tube is curved owing to surface tension [1]. The meniscus is concave or convex upwards as the liquid wets the solid container or does not wet the solid container and the value of angle of contact is acute or obtuse respectively [1]. The value of  $\theta$  for mercury with glass is  $140^\circ$  and that of water with glass is  $8^\circ$ .

As shown in Fig (5.1), the meniscus is assumed to be hemispherical in shape and the radius of curvature 'R' of the liquid surface is accordingly evaluated using the expression for the height 's' to which a liquid rises on meeting a solid. In general, when a free liquid meeting a plane vertical rigid wall, then in the two dimensional field, the height 's' to which the liquid climbs the rigid wall is given by the expression as under [2].

$$s^2 = 2F_t (1 - \sin \theta) / \rho g \quad (5.1)$$

where  $\theta$  is the angle of contact between the liquid and the solid (tube),  $\rho$  is the density of the liquid in  $\text{kg/m}^3$ ,  $g$  is the force of gravitational acceleration and is  $9.8 \text{ kg/m}^2$ ,  $F_t$  is the surface tension of the liquid.

Using the expression for 's' as explained above, the radius of curvature 'R' can be expressed in terms of the tube radius  $r$  and height  $s$  as under

$$R = (r^2 + s^2) / 2s \quad (5.2)$$

Thus equation 5.1 & 5.2 are used to determine the radius of curvature of the top of the liquid surface

Having obtained an expression for the radius of curvature of the liquid surface, in terms of other known parameters, now we will briefly consider the wave propagation of a gaussian beam in the next section.

## 5.2 Gaussian Beam Propagation

The normalized scalar electric field phasor (i.e.  $U(x, y, z)$ ) of a circularly symmetric gaussian beam at a distance 'z' from the output end of the source is given by [3] the expression

$$U(x, y, z) = \left( \frac{2}{\pi} \right) \exp \left( -jkz + j\Psi(z) \right) / w(z) \times \exp \left( - (x^2 + y^2) / w(z)^2 - jk (x^2 + y^2) / 2R(z) \right) \quad (5.3)$$

where  $k$  is propagation constant  $= 2\pi / \lambda$   $\Psi(z)$  is given by the expression

$$\Psi(z) = \tan^{-1} \left( z \lambda / \pi w(z)^2 \right) \quad (5.4)$$

and  $R(z)$  = the radius of curvature of the beam at a distance  $z$ . The spot size of the beam at a distance  $z$  is given by

$$w(z) = w_0 \sqrt{1 + \left( z \lambda / n_1 \pi w_0 \right)^2} \quad (5.5)$$

where  $w_0$  is the minimum spot size of the beam at  $z = 0$  as has been shown in Fig (5.2),  $n_1$  is the refractive index of the medium, and  $\lambda$  is the wavelength at which the laser diode is operating

From  $R(z)$  we can define a complex radius of curvature  $q(z)$  as [3]

$$1/q(z) \equiv 1/R(z) - j \lambda / \pi w(z)^2 \quad (5.6)$$

The above expression for a gaussian beam is significant because the light beam coming out from the laser diode can be treated to be a gaussian beam

### 5.3 Power Coupled to Photodiode from a Gaussian Beam in free space

The intensity of a circularly symmetric Gaussian beam at a distance  $z$  from the output end of the source is given by [ 4 ]

$$I(r,z) = (2P_s / \pi w(z)^2) \exp (-2r^2 / w(z)^2) \quad (5.7)$$

If the beam falls on a photodiode of radius ' $d$ ' and responsivity =1 the power coupled  $P_d$  is given by

$$P_d = \int_0^{2\pi} \int_0^d I(r,z) r dr d\theta \quad (5.8)$$

Integrating the above expression we get

$$P_d = P_s (1 - \exp (-2d^2 / w(z)^2)) \quad (5.9)$$

In equation (5.9) we have neglected the absorption loss inside the medium and any loss due to reflection at the medium - detector interface. Thus for a fixed value of  $d$  and  $P_s$ , the power received at detector  $P_d$  is a function of  $w(z)$  only.

Multiple reflections may take place between the glass top of the photodetector & the photodetector material but as these surfaces are not optically flat, so we do not consider multiple reflections between these two planes. Fresnel Reflection losses occur at the following interface

- (a) the liquid and the glass bottom of the container
- (b) the glass bottom of containers and the glass top of detector and
- (c) the glass top of photodetector and the photodetector material

As the Fresnel losses at these three interface are very small in comparison to the Fresnel Reflection losses which take place at the interface of the air and liquid, so we will consider the losses which take place at the interface of the air and the liquid, while evaluating the Fresnel Reflection losses

Taking into consideration the absorption losses as well as the Fresnel Reflection loss at the air liquid interface the power coupled  $P_d$ , in transmissive type of sensors (configuration No 1 and 2), is given by

$$P_d = T P_s (1 - \exp(-2d^2 / w_3^2)) \exp(-a h) \quad (5.10)$$

where  $a$  is the absorption coefficient per unit length inside the liquid at the operating wavelength,  $d$  is the radius of the detector,  $P_s$  is the source power,  $h$  is the height of liquid column and  $T$  is the loss due to Fresnel Reflection and is given by

$$T = 4 n_1 n_2 / (n_1 + n_2)^2 \quad (5.11)$$

Thus for a given value of  $d$ ,  $P_s$ ,  $w_o$ ,  $\lambda$ ,  $a$ ,  $n_1$  and  $n_2$  the power coupled varies with height of liquid column  $h$ , provided that the refractive index of the liquid ( $n_2$ ) remains constant

### 5.3.1 Power Coupled to Photodiode in an Offseted Detector

The expression for  $P_d$  as given by equation 5.9 is based on the assumption that there is no offset between the source and detector. While it may be possible to achieve this condition in case of the first two configurations (i.e. transmissive type of sensors), but in configuration no's 3&4 (i.e. reflective type of sensors) where both the source and detector are on the same side of the tube, it may not be possible. This is because even if the source and detector are kept adjacent to each other, still the center of the detector will be offset from the center of the source by a distance equal to the sum of the radius of the source and of the detector.

In reality, as shown in Fig 5.3, there is a fixed lateral offset ( $q_1$ ) between the centre of the source and detector. The least value of this offset is equal to the sum of the radii of the source and the detector assuming both are placed adjacent to each other. Mathematically  $q_1 = d_1 + d_2$  where  $d_1$  &  $d_2$  is the radius of the source and detector respectively. There can be lateral offset due to

**(a). Angular Misalignments** These are due to angular displacements namely

(i) A tilt in the liquid surface due to a tilt in the tube in which it is kept will result in a tilt in the level of the liquid surface and the light beam will undergo a transverse shift ' $q_2$ ' due to reflection

(ii) A fixed tilt offset caused by the misalignment of the light source and the photodiode during the fabrication of the sensor package (here after referred to as angular offset)

**(b). Linear Misalignment Effect.** There may also be a fixed lateral offset ' $q_1$ ' between the source and detector during the fabrication

The effect of all these three misalignments is that the optical beam is shifted in a transverse direction away from the centre of the photodiode. Without loss of generality we will consider the effects of these offsets in the x-z plane only. In this thesis, we will concern ourselves only with the effect of the fixed lateral offset ( $q_1$ ), which will hereafter be referred to as ' $q$ '

Now the power coupled to a photodiode is as given by equation 5.8 & equation 5.9 with the change that  $r^2 = ((x-q)^2 + y^2)$  where  $q$  is the offset

$$\text{thus } P_d = (2P_s / (\pi w(z)^2)) \int_0^{2\pi} \int_0^d \exp(-2((x-q)^2 + y^2) / w(z)^2) dx dy$$

which reduces to

$$P_d = (2P_s / (\pi w(z)^2)) \exp(-2q^2 / w(z)^2) \int_0^{2\pi} \int_0^d \exp(-2r^2 / w(z)^2) \exp(2rq \cos \theta / w(z)^2) r dr d\theta$$

(5.12)

On trying to evaluate this integral we get terms containing error function and the integral does not give a closed form expression. The above expression is integrated using NAG routine [4] (DOIDAF) based on the

method described by Patterson [5], [6] A programme was written in fortran language to evaluate the value of this integral and hence power coupled to the photodetector for different values of liquid level. The programme can be run by any user to generate data files by inputting various values of design parameters such as tube height  $h$ , tube width  $w$ , detector radius  $d_2$ , refractive index of liquid  $n_2$  and the value of the offset ' $q$ '

Taking into consideration the absorption losses as well as the Fresnel Reflection loss at the air liquid interface the power coupled to the detector is given by

(a) For configuration No 3 (both source & detector at top of tube)

$$P_{\text{det}} = R P_d \quad (5.13)$$

where  $R = (1 - T)$

(b) For configuration No 4 (both source & detector at bottom of tube)

$$P_{\text{det}} = R P_d \exp(-2a h) \quad (5.14)$$

where  $a$  is the absorption coefficient per unit length inside the liquid at the operating wavelength,  $d$  is the radius of the detector,  $h$  is the height of liquid column,  $T$  is the loss due to Fresnel Reflection and  $P_d$  is as given by equation 5.12. The coupling efficiency is defined as

$\eta = (P_d / P_s) 100$ , where  $(P_d)$  is as given by equation (5.10) for configuration no 1 & 2

$\eta = (P_{\text{det}} / P_s) 100$ , where  $(P_{\text{det}})$  is as given by equation (5.13) and (5.14) for configuration no 3 & 4

#### 5.4 First Configuration : Expression for Spot Size & Power for Sensor Configuration No 1

As shown in Fig (5.8), if some liquid of refractive index  $n_2$  partially fills up the gap of length  $z$  between the optical source and photodiode, then the optical beam will propagate partially through air (distance  $z - h$ ) and partly through a liquid column of height  $h$ . The light travelling from the bottom of the

tube thus encounters a concave dielectric interface whose ray matrix in terms of A,B,C,D parameters [ 7 ] is given by

$$\begin{bmatrix} 1 & 0 \\ \frac{(n_2 - n_1)}{n_2 R} & \frac{n_1}{n_2} \end{bmatrix} \quad (5 \ 15)$$

The detailed derivation of the above expression has been done in appendix B. In the above expression, R is the radius of curvature of the liquid and  $n_1$  &  $n_2$  are the refractive indices of air and liquid respectively

The complex beam parameters at various planes are as under [5]

$q_1$  - at plane 11' i.e. at the output of the laser diode

$q_2 (-)$  - at plane 22' i.e. above the air liquid interface ( as viewed from the top of the tube )

$q_2 (+)$  - at plane 22' i.e. below the air liquid interface ( as viewed from the top of the tube )

$q_3$  - at plane 33' i.e. at the input end of the detector

At plane 11' that is at source ( $z=0$ ) , the complex beam parameter  $q_1$  is given by [6]

$$1/q_1 = -j \lambda / n_1 \pi w(z)^2 \quad (5 \ 16)$$

where  $w_0$  is the size of gaussian beam measured at  $z=0$ . The transformed beam parameter  $q_2 (-)$  just to the left of the air liquid interface is given by  $q_2 (-) = q_1 + (z - b)$ . The beam parameter  $q_2 (+)$ , just below the air liquid interface is given by

$$q_2 (+) = \left[ \frac{Aq_2(-) + C}{Bq_2(-) + D} \right] \quad (5 \ 17)$$

where A, B, C, D are the elements of the ray matrix given by expression (5 15) Finally the beam parameter  $q_3$  at the liquid detector interface is given by

Finally the beam parameter  $q_3$  at the liquid detector interface is given by  $q_3 = (q_2(+) + h)$  Also,  $q_3$  is related to the beam spot size  $w_3$  and radius of curvature of the beam  $R_3$ , through the equation

$$1/q_3 = 1/R_3 - j\lambda/n_2\pi w_3^2 \quad (5 18)$$

From equations (5 16), (5 17) and (5 18), the expression for beam spot size at plane 33' is derived at appendix 'A' and is given by

$$w_3 = w_o \sqrt{(1 + (n_2/n_1)h/n_2 R)^2 + (g\lambda/n_1\pi w_o^2)^2} \quad (5 19)$$

$$\text{where } g = ((n_2/n_1)h/n_2 R + 1)(z - h) + (n_1/n_2)h$$

If the liquid is kept in a tube with a large diameter, the surface of the liquid is normally flat in shape. For a flat surface with no radius of curvature and the expression for beam spot size at plane 33' is given by

$$w_3 = w_o \sqrt{1 + (g\lambda/n_2\pi w_o^2)^2} \quad (5 20)$$

$$\text{where } g = h + (n_2/n_1)(z - h)$$

## 5.5 Expression for Spot Size & Power received for Sensor Configuration No 2

In this configuration the detector is at the top of the tube and the source is at the bottom as shown in Figure (5 10). A liquid of refractive index  $n_2$  partially fills up the gap of length  $z$  between the laser diode & the photodetector and the optical beam propagates a distance ' $h$ ' through the liquid and the remaining distance  $(z-h)$  through the air. The light travelling from the bottom of the tube thus encounters a convex dielectric interface whose ray matrix in terms of A, B, C, D parameters [7] is given by

$$\begin{bmatrix} 1 & 0 \\ \frac{(n_2 - n_1)}{n_1 R} & \frac{n_2}{n_1} \end{bmatrix} \quad (5.21)$$

Proceeding in the way we analyzed configuration no 1 in the previous section we can show that the expression for the spot size at the detector is given by

$$w_3 = w_0 \sqrt{(1 + (n_2 - n_1)(z - h) / n_1 R)^2 + (g \lambda / n_2 \pi w_0^2)^2} \quad (5.22)$$

$$\text{where } g = ((n_2 - n_1)h / n_1 R + n_2 / n_1)(z - h) + h \quad (5.23)$$

### 5.5.1 Total Internal Reflection Considerations

As in sensor configuration no 2, the light is travelling from a denser to a rarer medium and there is a possibility of total internal reflection and hence the cone of light actually passing through from denser to rarer medium may vary. We analyzed to discern whether there is any appreciable change in the spot size and the illumination cone, on going from denser to rarer medium, and the same is explained in the subsequent paragraph

As shown in Fig (5.5), a gaussian beam of light incident on a flat interface between two mediums is shown. Let  $\theta$  be the angle of the illumination beam incident on the liquid surface and  $\theta'$  is the angle of the 'fraction' of illumination beam which passes through to the rarer medium. The critical angle  $\theta_c = \sin^{-1}(n_1 / n_2)$ . Thus when  $\theta' > \theta_c$ , total internal reflection occurs. Thus  $\theta' \leq \theta_c$ , while considering the fraction of beam of light passing through the interface. Now for planar angles  $\theta$  &  $\theta'$ ,  $\tan \theta = r / R(z)$  and  $\tan \theta' = r' / R(z)$ . But for large distances  $R(z)$ , we can approximate the length of the arc subtended to be .

$$r = R(z) \theta \quad \text{and} \quad r' = R(z) \theta' \quad (5.24)$$

Also  $\theta' \leq \theta_c$  and  $\theta = \theta_{beam}$ , where  $\theta_{beam}$  is the far field beam angle [3] given by

$$\theta_{beam} = \lambda / \pi w_o \quad (5.25)$$

Using equations (5.24) & (5.25) we can show that for large  $z$ , the spot size  $w(z)$  is given by

$$w(z) \approx z \lambda / \pi w_o^2 n$$

Also for large distances  $z$ ,

$$r = (\sqrt{z^2 + y^2})^{1/2} = z \lambda / \pi w_o^2 n \quad \text{Thus for far field } z \geq \pi w_o^2 n, \quad r \approx w(z)$$

From equation 5.24 & 5.25 we can show that  $r' = r \theta_c / \theta_b$ . But as  $r \approx w(z)$ , thus

$$w(z)' = w(z) \theta_c / \theta_b \quad (5.26)$$

where  $w(z)$  is the actual spot size of the beam at a distance  $z$  in any single medium and  $w(z)'$  is the actual spot size at a distance  $z$  if the beam travels from a denser to a rarer medium. Substituting for  $w(z)$  and  $\theta_c$  we get

$$w(z)' = \theta_c (\pi w_o^2 n) / \lambda w_o \sqrt{1 + (z \lambda / n_1 \pi w_o^2)^2} \quad (5.27)$$

Numerically substituting the values of various constants and variables in the expression for far field distance ' $z$ ' and for  $\theta_b$  we obtain certain results which are tabulated at table 5.1 & table 5.2 respectively and the inferences drawn from them are stated in the subsequent paragraphs

From equation (5.27) we had the relation  $w(z)' = w(z) \theta_c / \theta_b$ , which means that  $w(z)'$  will be a fraction of or a percentage of  $w(z)$  only in the case when  $\theta_b$  is  $> \theta_c$ . In all other cases, so long as  $\theta_c > \theta_b$ , the complete beam will pass through the interface, into the rarer medium

From the results tabulated we find that  $\theta_b$  is very small compared to  $\theta_c$  and for the range of values over which the optical sensor would be designed to function, it is seen that  $\theta_b$  is at best =  $8.63^\circ$  and corresponding to that, the far field is  $6.6 \mu m$ , that is a very small distance compared to the tube length

Thus we may assume that most of the gaussian beam of light would pass through from the liquid to air in configuration no 2 and undergoes refraction governed by the ray matrices for the spherical dielectric interface. The final spot size in sensor configuration no 2 will be as given by equation (5.22)

The power coupled to the photodiode is as given by the equation (5.10) which is reproduced below

$$P_d = T P_s (1 - \exp(-2d^2 / w_3^2)) \exp(-ah)$$

where  $a$  is the absorption coefficient per unit length inside the liquid at the operating wavelength,  $h$  is the height of liquid column,  $T$  is the loss due to Fresnel Reflection,  $d$  is the radius of the detector &  $P_s$  is the source power. Fresnel Reflection losses occur at the interface between (a) the glass bottom of container and the top of laser diode, (b) the air and the glass top of the photodetector, and (c) the glass top of photodetector and the photodetector material but these are very small in comparison to the Fresnel Reflection losses which take place at the interface of the air and liquid & air.

### 5.6 Expression for Spot Size and Power received for Sensor Configuration No 3

In this sensor configuration both the source and detector are at the top of the tube as shown in Figure (5.12). The light travelling from the top of the tube thus encounters a liquid surface which acts like a concave reflecting surface of radius of curvature  $R$  whose ray matrix in terms of  $A, B, C, D$  parameters [7] is given by

$$\begin{bmatrix} 1 & 0 \\ \frac{-2}{R} & 1 \end{bmatrix} \quad (5.28)$$

provided  $R > 0$  Proceeding in the way we analyzed configuration no 1 in the previous section we can show that the expression for the spot size at the detector is given by

$$w_3 = w_o \sqrt{(1 - 2(z - h) / R)^2 + (2(z - h)\lambda / n_1 \pi w_o^2)^2 (1 - (z - h) / R)^2} \quad (5.33)$$

where  $h$  is the height of liquid column from the bottom of the tube .The power coupled to the photodiode is as given by the equation 5.13 explained earlier

### 5.7 Expression for Spot Size and Power received for Sensor Configuration No 4

In this sensor configuration both the source and detector are at the bottom of the tube as shown in Figure (5.13) . The light travelling up from the bottom of the tube encounters a liquid surface which acts like a convex reflecting surface of radius of curvature  $R$  , and gets reflected from it . The ray matrix of the convex reflecting surface in terms of A,B,C, D parameters [ 7 ]is given by

$$\begin{bmatrix} 1 & 0 \\ \frac{2}{R} & 1 \end{bmatrix} \quad (5.35)$$

provided  $R > 0$  Proceeding in the way we analyzed configuration no 1 in the previous section we can show that the expression for the spot size at the detector is given by

$$w_3 = w_o \sqrt{(1 + h / R)^2 + (2h\lambda / n_2 \pi w_o^2)^2 (1 + 2h) / R)^2} \quad (5.39)$$

where  $h$  is the height of liquid column

### 5.8 Summary

In this chapter we have analyzed the four configurations of a low cost optical sensor using physical optics considerations . We have derived expressions for the spot size available at the detector and the power received by the detector in all the four cases and programmes have been written to evaluate the power coupled to the photodetector and hence its coupling efficiency ,for different values of liquid

level We have also analyzed the total internal reflection considerations in case of configuration no 2 In the next chapter we will input numerical values for the various design parameters in the programmes and generate data files to plot the variation in the coupling efficiency with respect to the liquid level is plotted in each of the four configurations

## REFERENCES

- 1 K.L Gombar &K L Gogia "Fundamentals of Physics ", Pradeep publications Jalandhar 1998
- 2 G.K Batchelor , "An Introduction to Fluid Dynamics ", Cambridge University Press, London , 1967, chapter 1
- 3 A.E Seigmann , " An Introduction to Lasers and Masers ", Mc Graw Hill Series, 1971, chapter 16 &17
- 4 NAG Fortran Library Routine Document, Mark 14, - D01DAF
- 5 T N L Patterson, "The optimum addition of points to quadrature formulae ", Math comp 22, pp 847-856 ,1968 Errata, Math. Comp 23, p 892, 1969
- 6 T N L Patterson, "On some Gauss and Lobatto based integration formulae ", Math comp 22, pp 877 - 881 ,1968
- 7 B.Saleh and M Teich, " Fundamentals of Photonics ", John Wiley & Sons Inc, New York, chapter 3
- 8 A.K Ghosh and P K Paul, " A low cost optical liquid level sensor for liquid level measurement ", Applied Optics, vol 36, pp 6256-6263, Sep 1997
- 9 A Yariv , "Optical Electronics ", Holt ,Rinehart and Winston ,New York.1985,chapter 2,p32
- 9 A. Yariv, "Optical Electronics ", Holt, Rinehart and Winston, New York. 1985, chapter 2,p52
- 10 A E Seigmann , " An Introduction to Lasers and Masers ", Mc Graw Hill Series , 1971, Table 15 1(c) ,p5

**TABLE 5.1**

Variation in far field  $z \geq (\pi w_0^2 n / \lambda)$  for various values of  $w_0$  and  $\lambda$

Far Field $z \geq (\pi w_0^2 n / \lambda)$					
$\lambda \downarrow w_0 \rightarrow$	$1 \mu m$	$5 \mu m$	$10 \mu m$	$20 \mu m$	$40 \mu m$
$0.4 \mu m$	$10 \mu m$	$261 \mu m$	umm	4.17 mm	16.71 mm
$0.63 \mu m$	$6.6 \mu m$	$165.8 \mu m$	0.66 mm	2.65 mm	10.61 mm
$0.7 \mu m$	$5.96 \mu m$	$149 \mu m$	0.596 mm	2.38 mm	9.55 mm

**TABLE 5.2**

Variation in half beam angle  $\theta_b$  for various values of  $w_0$  and  $\lambda$

$$\theta_b^\circ = \theta_b \text{ (in radian)} (180/\pi) \text{ where } \theta_b \text{ (rad)} = \lambda / w_0 n \pi$$

$\lambda \downarrow w_0 \rightarrow$	$1 \mu m$	$5 \mu m$	$10 \mu m$	$20 \mu m$	$40 \mu m$
$0.4 \mu m$	$5.48^\circ$	$1.09^\circ$	$0.0548^\circ$	$0.27^\circ$	$0.14^\circ$
$0.63 \mu m$	$8.63^\circ$	$1.72^\circ$	$0.86^\circ$	$0.43^\circ$	$0.22^\circ$
$0.7 \mu m$	$9.59^\circ$	$1.91^\circ$	$0.96^\circ$	$0.48^\circ$	$0.24^\circ$

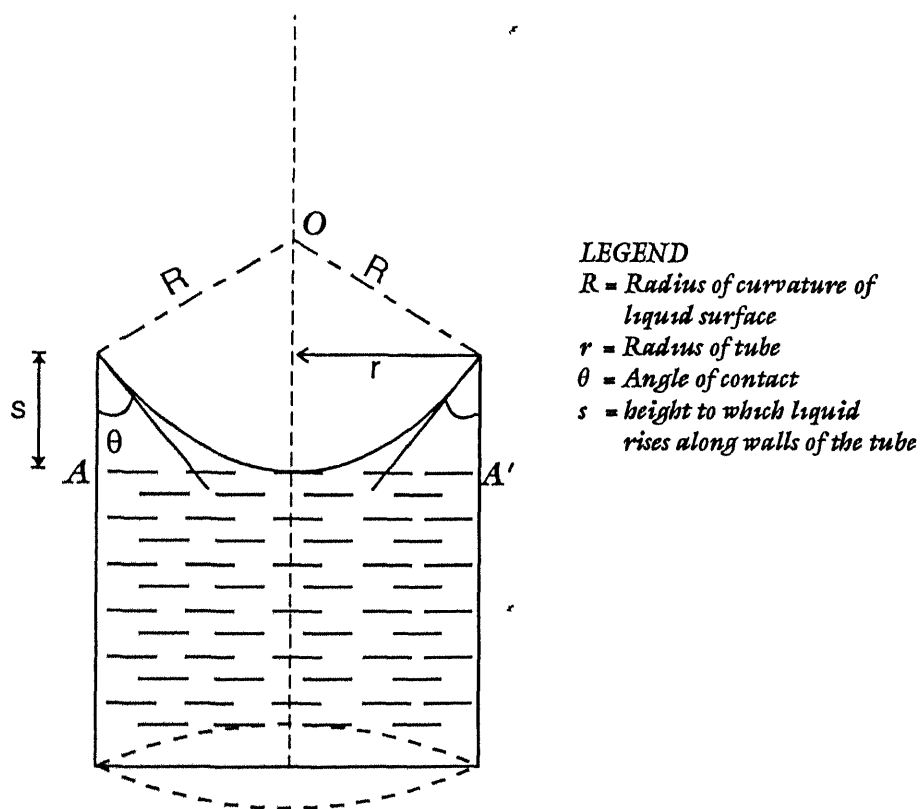


*Fig. 5.1 Radius of Curvature of liquid surface*

**CENTRAL LIBRARY**  
**I. I. T., KANPUR**  
**No. A 127828**

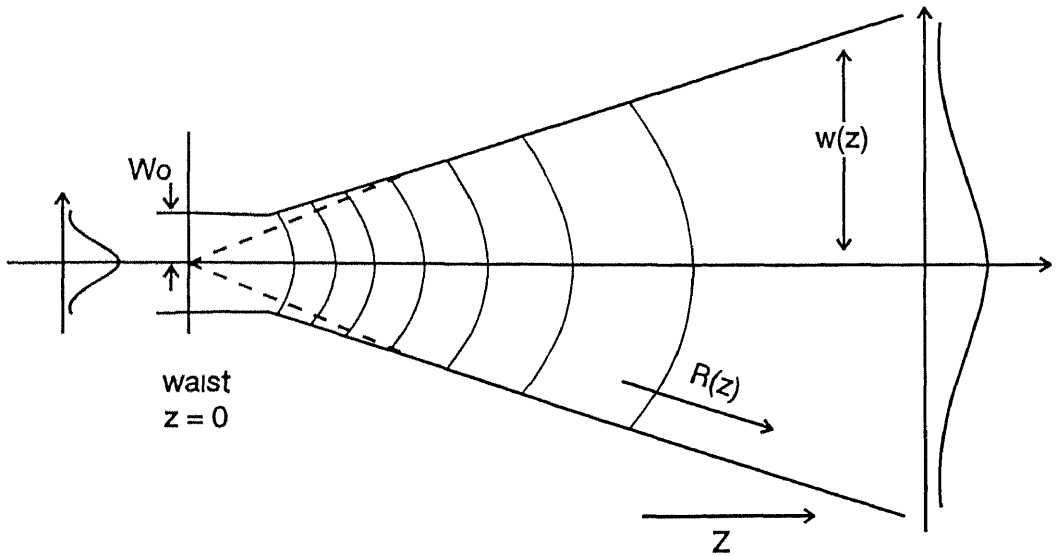


*Fig. 5.2 Notation for a lowest order gaussian beam diverging away from its waist*

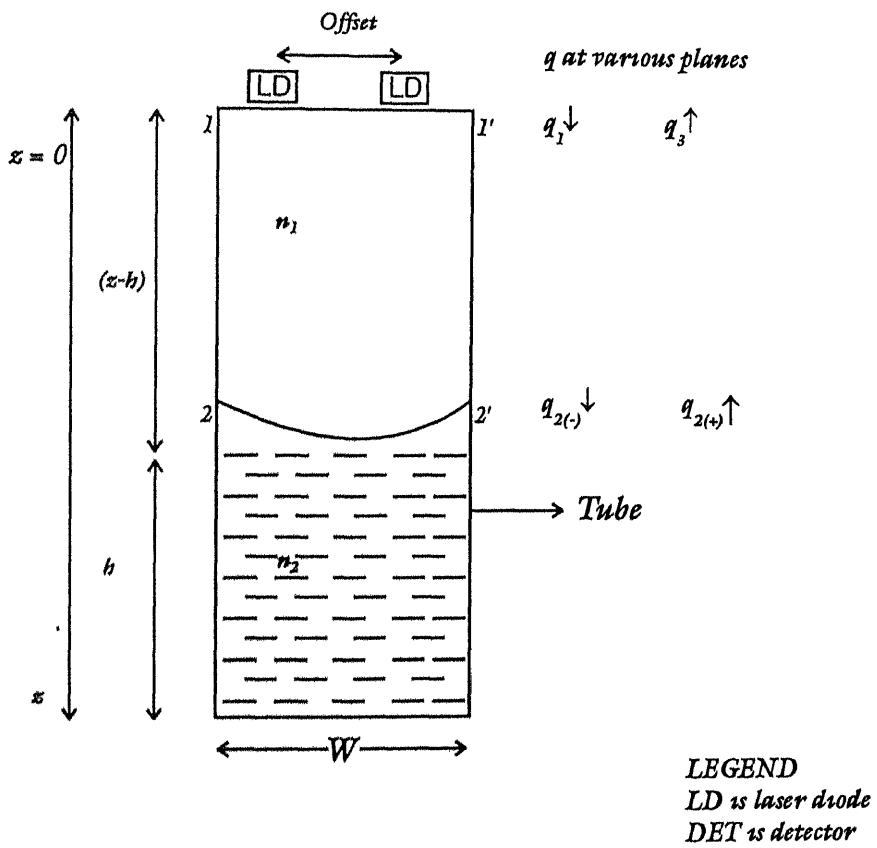


*Fig. 5.3 The detector at an offset from the source*

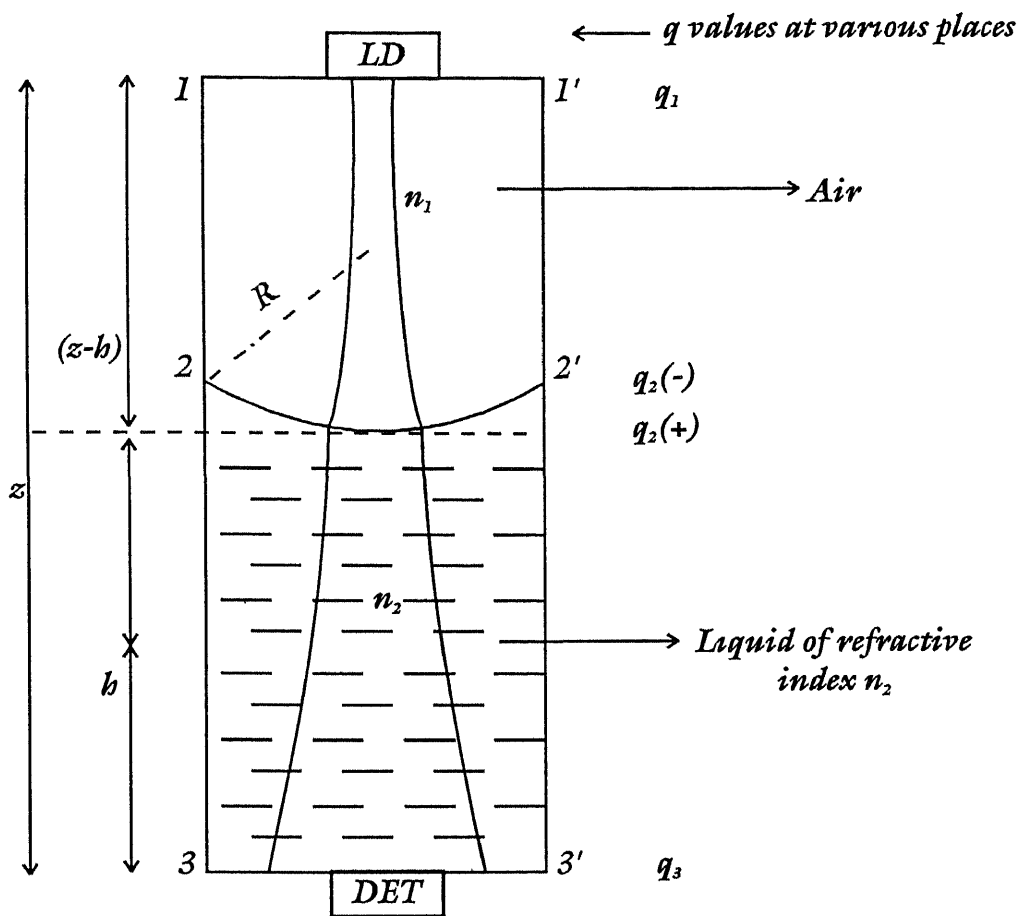


Fig. 5.4 Spot size analysis for configuration No. 1

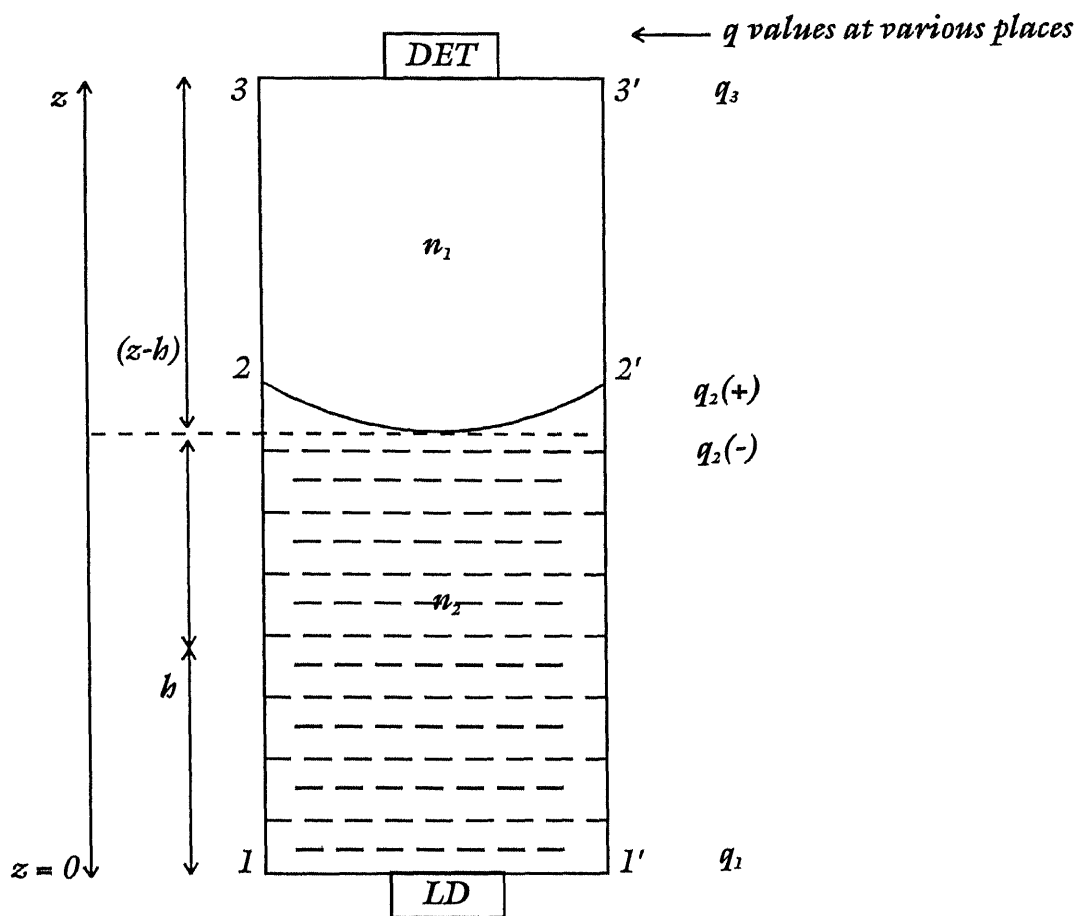


Fig. 5.5 Configuration No. 2

$\theta$  is half beam divergence angle  
at which light is incident

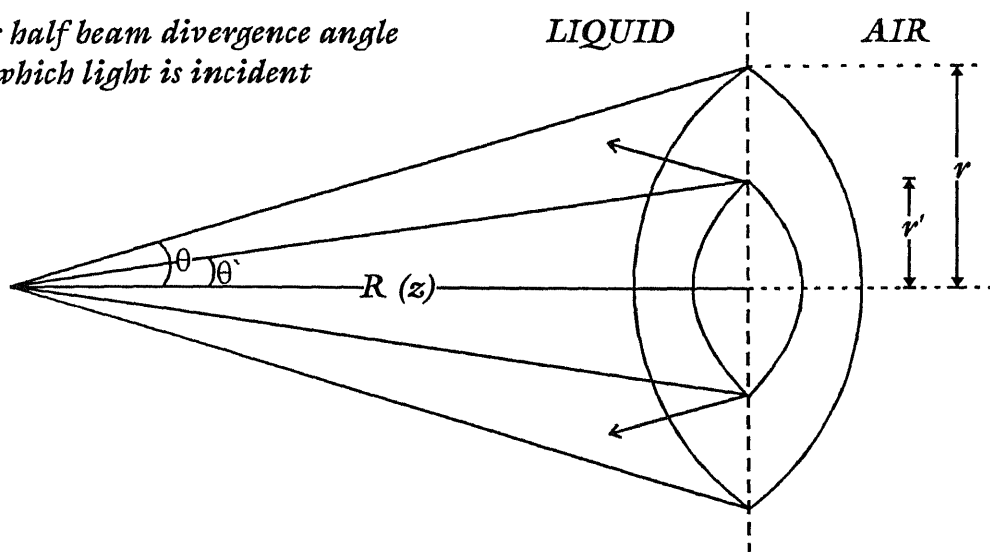
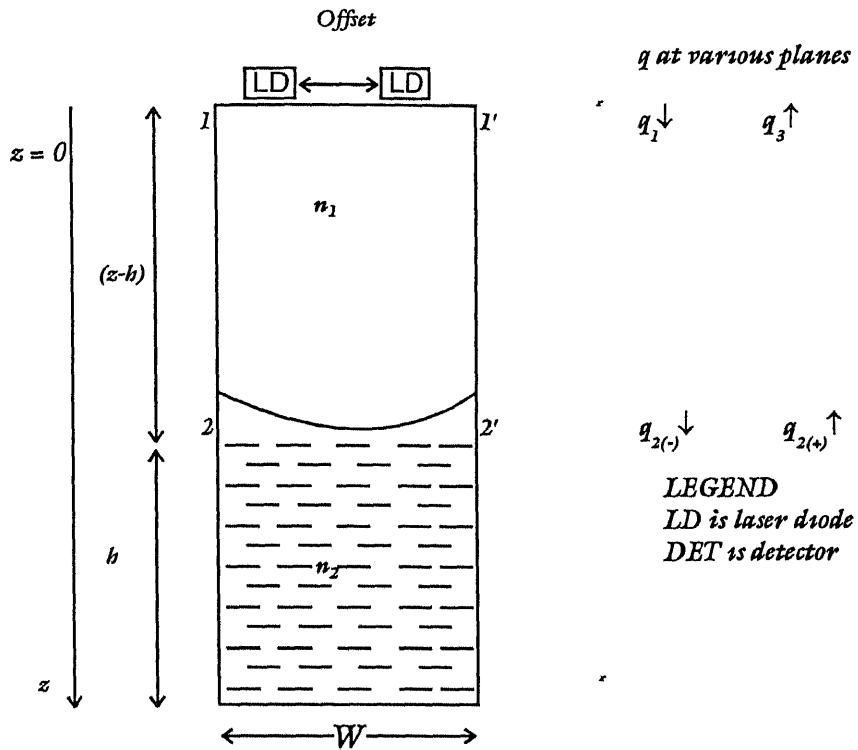


Fig. 5. Total internal reflection condition analysis for configuration No. 2



*Fig. 5.7 Sensor configuration No. 3*

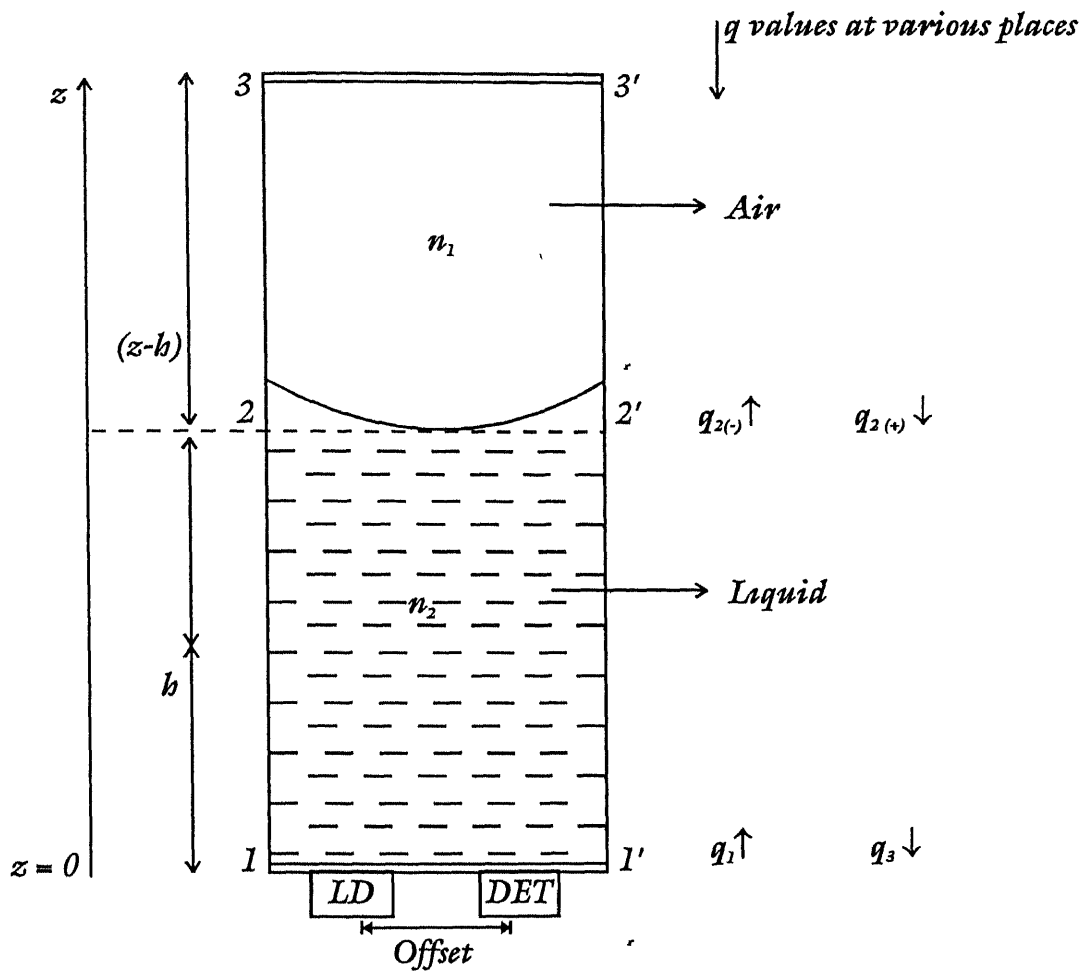


Fig. 5.8 Sensor configuration No. 4

## **CHAPTER 6**

### **SIMULATION RESULTS**

In the previous chapter we derived expressions for the spot size available at the detector and the power received by the detector in all the four configurations of an optical sensor. Programmes to evaluate the power coupled to the photodetector and hence its coupling efficiency, for different values of liquid level have also been written. In this chapter we will select various design parameters and input their values in the programmes to generate data files. These data files will be used to plot the variation in the coupling efficiency with respect to the liquid level in each of the four configurations. Finally, we carry out a comparative analysis of the results obtained from the simulation of all the four configurations, with an aim to select a feasible model from amongst them.

#### **6.1 Analysis of the Results**

**6.1.1 Test Data Used** Various design parameters which have to be selected are as follows

- (a) Diameter of tube
- (b) Height of tube
- (c) Refractive index of liquid
- (d) Radius of detector
- (e) Radius of source
- (f) Wavelength of laser diode
- (g) Waist spot size at give wavelength

- (h) Output power of source
- (j) Absorption coeff /mm at given wavelength
- (k) Surface tension of liquid
- (l) Angle of contact of liquid with solid
- (m) Density of liquid

There is a requirement for an optical window to be put on the base of the tube for transmissive type of sensors (sensor configuration No's 1 and 2) Optical windows come in specified sizes and due to the complexity in their fabrication process, their cost increases as their size becomes larger. For our low cost optical sensor, the optical window should be large enough to accommodate the source and detector. Thus an optical window with a diameter of approximately an inch (25.4 mm) would suffice for our purpose. Keeping a margin of 1.2 mm on either side of the diameter to allow for fixing the optical window to the walls of the tube, at the base of the tube we are left with an optical window with a diameter of 23 mm.

The tube in which the liquid is kept though should not be so long that it becomes unwieldy to handle, yet it should be long enough to allow proper measurement of the liquid level by our optical sensor. In view of this, a tube of length = 10 cm (100 mm) would meet the requirement. Moreover, the range over which the sensor should be able to function should be starting from 5 mm from the base of the tube to 10 mm short of the top of tube. In view of this, a tube of length = 11.5 cm (115 mm) would meet the requirement as this would allow measurement to be done over a range of 10 cm (100 mm). Moreover, Hindustan Aeronautics Limited (Lucknow) had also projected the requirement that the liquid measurement should be possible over a length of 10 cm [4].

The liquid selected for the purpose of our analysis is water and the refractive index, absorption coefficient, density and the angle of contact has been accordingly selected as 1.33,  $7.6 \times 10^{-3}$ ,  $1000 \text{ kg/m}^3$  and  $8^\circ$  respectively.

Looking through the data sheets of various low cost laser diodes in the visible region (at a wavelength of say 670 nm), the radius was about 1 to 2 mm. The power output of such laser diode can be in the range of 1- 2 mW, which is adequate for the requirement of our optical sensor. The minimum spot size of the gaussian beam at the operating wavelength is 100 microns. These lasers are available with simple optics to convert the beam to a circular spot. The list of design parameters thus selected is tabulated at table 6.1

### 6.1.2 Variation in Power and Coupling Efficiency

The graphical plots of the variation in the coupling efficiency for sensor configurations no's 1,2 and 3 are shown in Fig's 6.1, 6.2 and 6.3 respectively. Sensor configuration no 4, in which both the laser diode and the detector are at the bottom of the tube has been discarded at the outset as its coupling efficiency was between 0.24% to 0.34%, which is very small in comparison to the coupling efficiency achieved in the other 3 configurations. The reason for this rather low coupling efficiency is because in configuration no 4, the absorption inside the liquid is double the loss in case 1 and 2.

It is seen from the plots in Figs 6.1 and 6.2 that in case of the configuration no's 1 and 2, the power decreases continuously as the liquid level ( $h_1$ ) is increased. This is because the detector, being aligned with the source and placed in the centre of the tube will always fall within the cone of light being sent by the Laser Diode. With an increase in  $h_1$ , the cone of light is spread over a larger area thus the intensity of light being received at detector decreases. Also, the absorption loss increases with  $h_1$ .

The variation of power coupling efficiency (Eff) in the graph is linear throughout. But in the region between  $h_1 = 10$  mm to  $h_1 = 85$  mm, the power coupling efficiency is reasonably in both these configurations. Thus both these configurations can be used for measuring level in this region. With the radius of detector chosen as 2 mm the range of variation in coupling efficiency, is from 14 % to 77 %, for sensor Configuration no 1 and from 42% to 61% for Configuration no 2. However, when the radius of the

detector is increased to 4 mm, the range of variation in coupling efficiency, for Configuration no's 1 and 2 is from 43 % to 96% and from 42% to 93% respectively

The variation in coupling efficiency vs liquid level for configuration no 3, was plotted keeping the radius of detector and source at 2 mm and 1mm respectively. The offset is kept at the minimum value of 3 mm (i.e.  $q = d_1 + d_2$ ). On analysis of Fig 6.3, it is found that the response can be divided into two regions - the front slope and the back slope. The front slope of the plots pertains to the region of partial overlap between the detector and the cone of light reflected from the liquid surface and the back slope of the plot pertains to the region of complete overlap.

The coupling efficiency increases with  $h_1$  in the region of front slope. This is due to the fact that initially, as the liquid level increases, the intensity of light coupled to the detector increases thus the power coupled to detector ( $P_d$ ) and the power coupling efficiency (Eff) increase. After a certain liquid level, the light reflected from the liquid surface falls on the complete area of the detector and maximum  $P_d$  and Eff are achieved. After this stage, though there is no further increase in the area of the detector which receives light, yet the intensity of light falling per unit area decreases and thus  $P_d$  and Eff decrease and this is the region of back slope of the plot.

## 6.2 Selection of a Feasible Design for an Optical Sensor

On comparing the results obtained and considering the practical problems associated with the proposed design, we come to the under mentioned conclusions

(a). **Sensor configuration no 4** (both source and detector at the bottom), can be discarded as it involves maximum absorption losses because the liquid travels up and down inside the liquid column.

(b). **Sensor configuration no's 1 and 2**, though provide 40% to 97% coupling efficiency, yet suffer from the following drawbacks

(i) In the presence of suspended particles in the liquid, the absorption per unit distance inside the liquid will vary because the presence of suspended particles makes the liquid non-homogeneous in nature

(ii) These types of sensors are prone to misalignment errors and alignment considerations are very critical in these sensors

(iii) From the packaging aspect, it is preferable to place both the source and detector together in a compact housing. But in configuration no 1 and 2 the source and detector are at opposite ends of the device containing the liquid

(iv) It is practically difficult to place any component (laser diode or detector) at the bottom of the tube

**(c). In sensor configuration no 3** (both source and detector on top of the tube), the power received at the detector is less as compared to that in configuration no 1 and 2 and the coupling efficiency in the region of back slope, varies from 1% to 14%. Despite this obvious disadvantage, this type of sensor has certain advantages, which are as under

(i) For a given liquid kept in a container of a specified solid material, the shape of the liquid meniscus will not vary over a period of time and thus the pattern of the light being reflected from its surface will not vary with time

(ii) Impurities that contaminate the liquid are of two types - suspended impurities and impurities that float. The floating variety can be separated from the liquid easily by various mechanical means. Even if suspended impurities are there in the liquid, then due to gravity they are likely to settle down and would not float on the surface. Thus the reflection from the surface is uniform and there is no variation in power received at the detector, for a particular liquid, because of impurities in the liquid.

(ii) As both source and detector are on top of the tube, so it is easier from the aspect of packaging and manufacturing because the electronic circuitry associated with laser diode and detector can be placed together at one place

(iv) Electronically we can detect signals in the range of nano amps. The photocurrent from the detector in this configuration is in the range of micro amps to nano amps and is sufficient to be detected by the electronic circuitry.

In view of the above, sensor configuration no 3 was selected as a feasible design for a low cost optical sensor. In the next section we will discuss the various types of misalignments that can take place in an optical liquid level sensor.

### 6.3 Effects of Variation in Various Parameters

To appreciate the effect of the various design parameters on the coupling efficiency, keeping all other design parameters the same, one particular parameter was varied and its effect was analysed. The effect variation of various parameters has been considered and the analysis of the same is given in the subsequent paragraphs.

In Fig 6.4, coupling efficiency with respect to liquid level  $h_1$  has been plotted for values of offset varying from 3 mm, 4 mm, 5 mm and 6 mm, for a given radius of the detector ( $d_2=2$  mm).

I. As the offset  $q$  is made to vary from 3 mm to 4 mm, 5 mm and 6 mm, efficiency decreases sharply with an increase in offset because as  $q$  increases, the amount of light being coupled to detector decreases. This is because the cone of light reflected by the liquid surface partially covers the detector. The coupling efficiency is maximum when the offset is minimum and is 3 mm (i.e.  $q = d_1 + d_2$ ). It is also seen that as the offset is increased, the dead zone of the sensor decreases and the effective range over which sensing is possible decreases.

The radius of the detector ' $d_2$ ' was varied from 2 mm to 5 mm, in steps of 1 mm and a plot of Eff vs  $h_1$ , for each variation was taken. While taking these plots, the offset was kept to the minimum possible value corresponding to the upper limit of variation in  $d_2$ . The same is shown in Fig 6.5. Similar observations were made as seen in the case of fig 6.4. Eff decreases with an increase in the offset. However, it is seen that these graphs that the reverse slope changes uniformly and is suitable for sensing purposes.

It is also seen that for the same offset, Eff increases as the radius of detector is increased. This is because with an increase in  $d_2$ , the area of detector increases and thus more light intensity can be coupled to it, for the same offset. Thus for an offsetted detector based optical sensor, ideally the offset should be kept to the minimum, that is equal to the sum of the radius of the source and the detector, and the radius of the detector should be large.

The waist spot size is varied from 0.1mm, 0.25mm, 0.5mm and to 1mm and the variation in coupling efficiency with respect to the liquid level is plotted as shown in Fig 6.6. It is seen that efficiency increases with an increase in the waist spot size as more power is being coupled to the detector. It is also seen that as waist spot size increases, the range of the sensor increases and there is a smaller dead zone where our optical sensor will be unable to sense the level of the liquid.

The values of the refractive index of three fluids were selected to study the variation in coupling efficiency with respect to liquid level. As shown in Fig 6.7, there is only a slight amount of variation in the coupling efficiency on varying the value of refractive index of the liquid. It is seen that efficiency decreases with an increase in the refractive index of the liquid. This is because with an increase in the value of  $n_2$ , the Fresnel Coefficient decreases and thus  $P_d$  and Eff decrease. Also, the variation in final spot size is dependent on the value of the refractive index of the liquid, which affects the final spot size, which in turn affects the coupling efficiency.

On varying the diameter of the tube, there is a change in the radius of curvature of the liquid surface, which in turn affects the coupling efficiency. From Fig 6.8 it is seen that as tube diameter is increased, which implies that as the liquid surface tends to become flat, the maximum amount of power gets

coupled to the detector at a lesser value of liquid level. This is due to the dependence of the spot size on the value of 'R'.

It is also seen that as the value of tube diameter (and thus R) increase, the gradient of back slope of the plot between coupling efficiency and liquid level becomes gradual and is suitable for the purpose of sensing.

#### 6.4 Annular Detector based Optical Sensor

An offsetted detector based optical sensor suffers from the disadvantage that it is less efficient as compared to an optic sensor with no offset. Also, the offset is prone to vary over prolonged operation and thus the sensor is required to be recalibrated periodically. To do away with the need to incorporate this offset, a design of an Annular detector based optic sensor has been proposed in this section.

Shown in Fig 6.9 is an annular detector with an outer radius =  $d_2$  and inner radius =  $d_1$ , with the source placed in the centre of the annular ring. Now the power coupled to a photodiode is given by

$$P_d = \int_0^{2\pi} \int_{d_1}^{d_2} I(r, z) r dr d\theta$$

$$\text{where } I(r, z) = (2 P_s / (\pi w(z)^2)) (\exp(-2 r^2 / w(z)^2)) \quad (6.1)$$

Integrating we get

$$P_d = P_s \{ \exp(-2 d_1^2 / w(z)^2) - \exp(-2 d_2^2 / w(z)^2) \} \quad (6.2)$$

Taking into account the Fresnel Reflection loss, the final expression for power is

$$P_d = P_s R (\exp(-2 d_1^2 / w(z)^2) - \exp(-2 d_2^2 / w(z)^2)) \quad (6.3)$$

where  $T = 4 n_1 n_2 / (n_1 + n_2)^2$  and  $R = (1 - T)$

Four different sizes of annular detector are taken with the inner radius fixed at 1 mm and the outer radius ' $d_2$ ' varied from 2 mm to 5 mm, in steps of 1 mm. The coupling efficiency of detector (Eff) is plotted against the liquid level for a tube of length = 115 mm and plots, as shown in Fig 6 10, are seen. It is observed that as  $d_2$  increases, coupling efficiency increases as the area of the detector increases. It is also seen that as the value of ' $d_2$ ' increases, the gradient of back slope of the plot between coupling efficiency and liquid level becomes gradual and is suitable for the purpose of sensing, though in this case the range of the sensor decreases and dead zone increases.

However, the most important aspect observed is that the front slope in the case of the plots for an annular detector is more gradual and is over a longer range of  $h_1$  as compared to that seen in Fig 6 3(a case of lateral offset  $q$ ). Thus the sensor is able to operate over a greater range, if an annular detector is used in the optical sensor.

## 6.5 Responsivity and Dead Zone of an Annular Ring Shaped Detector

As brought out from Fig 6 10, the response of an annular ring shaped detector is different from that of a detector with an offset and it has thus to be calibrated accordingly.

This type of detector has a uniformly varying front slope, which can be used for sensing. From Fig 6 18 and Fig 6 19 it is seen that for a specific  $d_2/d_1$  ratio, a larger value of  $d_1$  gives us a greater back slope over which sensing may be carried out.

The variation in Eff with respect to  $h_1$  can be detected till the 100mm mark, which is approximately 20% more than the range over which the offsetted detector can sense the variation in liquid level. It also meets our specifications in that it can almost sense over the complete range from 5mm to 105mm. Beyond the 100mm liquid level, this detector is unable to sense and the region from 100mm to 105mm is the 'dead zone' for the detector and sensing is not possible over this region.

Using equation (6 3) and differentiating with respect to  $h_1$ , to find the condition for occurrence of maxima we get the under mentioned relationship

$$d_2^2 = d_1^2 ( \exp ( 2 / w(z)^2 ( d_2^2 - d_1^2 ) ) ) \quad (6 4)$$

$$(M^2 / r^2) x^4 - (2 M^2 / r) x^3 + (M^2 - (4/r^2)) x^2 + (4/r) x - 1 = 0 \quad (6 5)$$

where  $x = (h - h_1)$ ,  $M = (2 \pi / \lambda n_1 w_0^2)$ ,  $\lambda$  is the wavelength of the light emitted by the source and  $w_0$  is the waist spot size of the beam

Equation (6 5) is a fourth order polynomial and we write a program in FORTRAN using NAG routine 'CO2AGF' [2] to calculate the roots of the polynomial which gives us the condition for occurrence of the maxima

## 6.7 Reduction of Effect of Offset

In this chapter we have considered the offset which exists between the source and the detector and derived an expression to calculate power and coupling efficiency at the detector, taking it into account. The response of an offsetted detector was analysed. An annular ring shaped detector was proposed which removes the need to introduce an offset. Using this detector, an expression to calculate power and coupling efficiency at the detector was derived. The response of this detector was analysed and the conditions for occurrence of maxima in this case were derived.

To reduce the effects of these lateral and angular misalignments on power coupling efficiency, we may use an array of photodiodes to detect the optical signal, instead of using a single photodiode [3]. The detector array so designed may contain  $(2m+1)$  identical elements, where  $m$  is a positive integer. We assume that the central photodiode  $m = 0$  is perfectly aligned with the optical source. The photocurrents from each photodiode are added together to form the net output signal.

## REFERENCES

- 1 S S Sekhon, M.Tech thesis on " Design of Reflective Fibre Optic Sensors for Displacement measurement", Department of Laser Technology, I I T Kanpur, 1998
- 2 NAG Fortran Library Routine Document, Mark 14, -C02AGF
- 3 A.K.Ghosh and P K Paul," A low cost optical liquid level sensor for liquid level measurement ", Applied Optics vol 36, pp 6256-6263, Sep1997
- 4 S Bhattacharya, HAL Lukhnow Private Communications

**TABLE 6.1****LIST OF DESIGN PARAMETERS SELECTED**

1	Diameter of tube	23 mm
2	Height of tube	115 mm
3	Refractive index of liquid	1.33
4	Radius of detector	2 mm
5	Radius of source	1 mm
6	Wavelength of laser diode	670 nm
7	Waist spot size at give wavelength	100 microns
8	Output power of source	2 mW
9	Absorption coeff /mm at given wavelength	$7.6 \times 10^{-3}$
10	Surface tension of liquid	$72.91 \times 10^{-3} \text{ N/m}^2$
11.	Angle of contact of liquid with solid	8 degrees
12	Density of liquid	$1000 \text{ kg/m}^3$

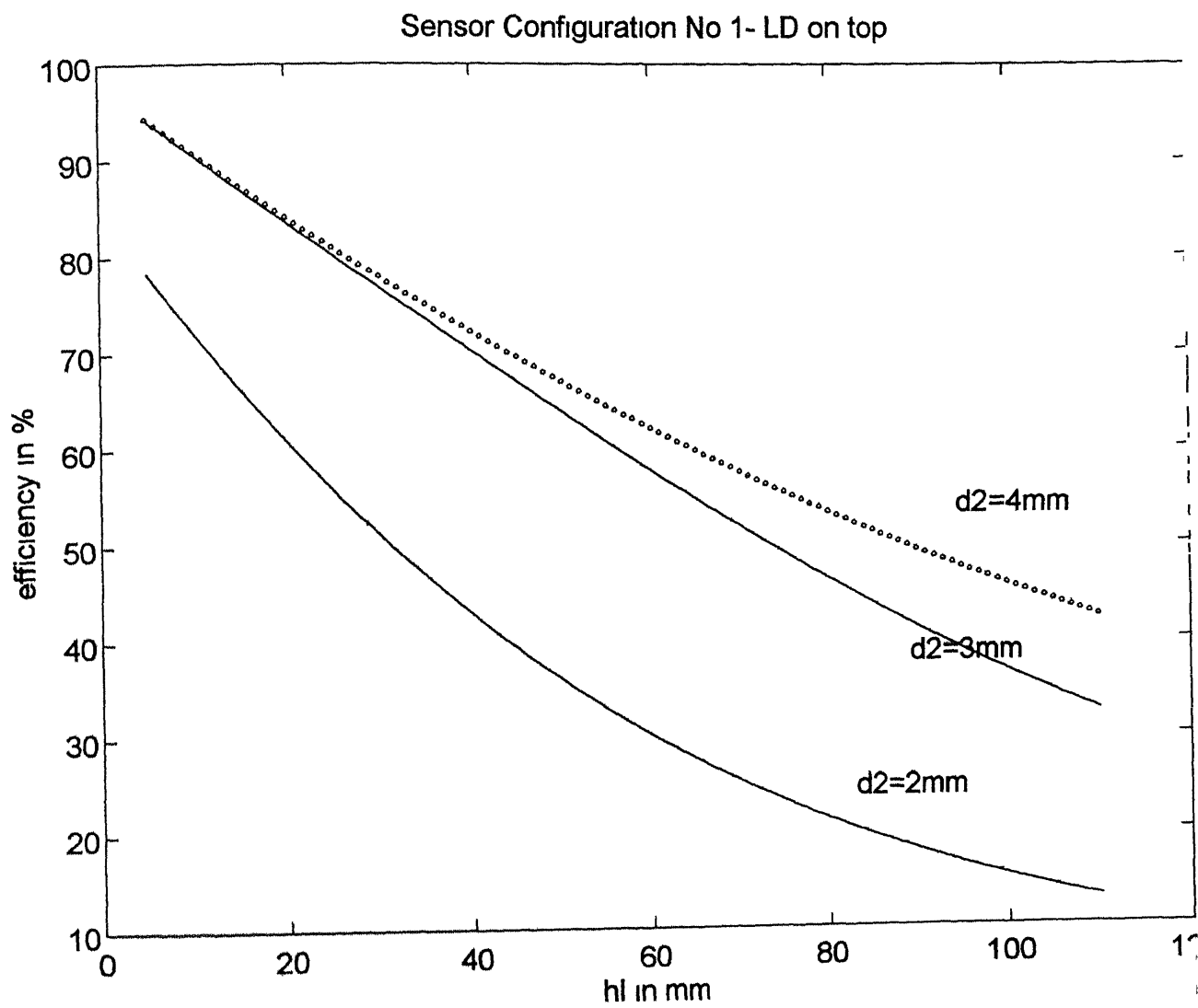


Fig 6.1 Coupling Eff vs Liq level, for variation in radius of detector

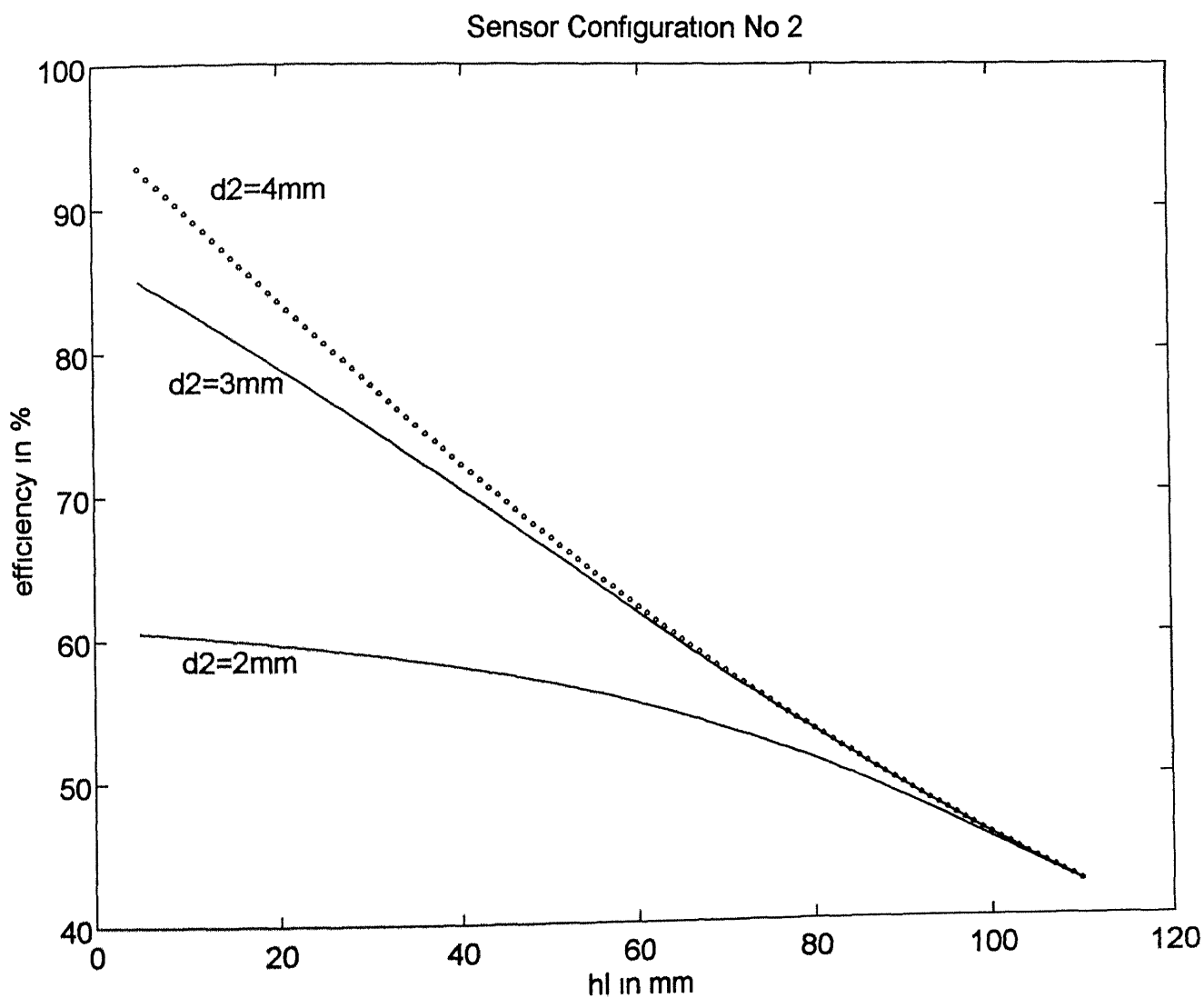


Fig 6 2 Coupling Eff vs Liq level, for variation in radius of detector

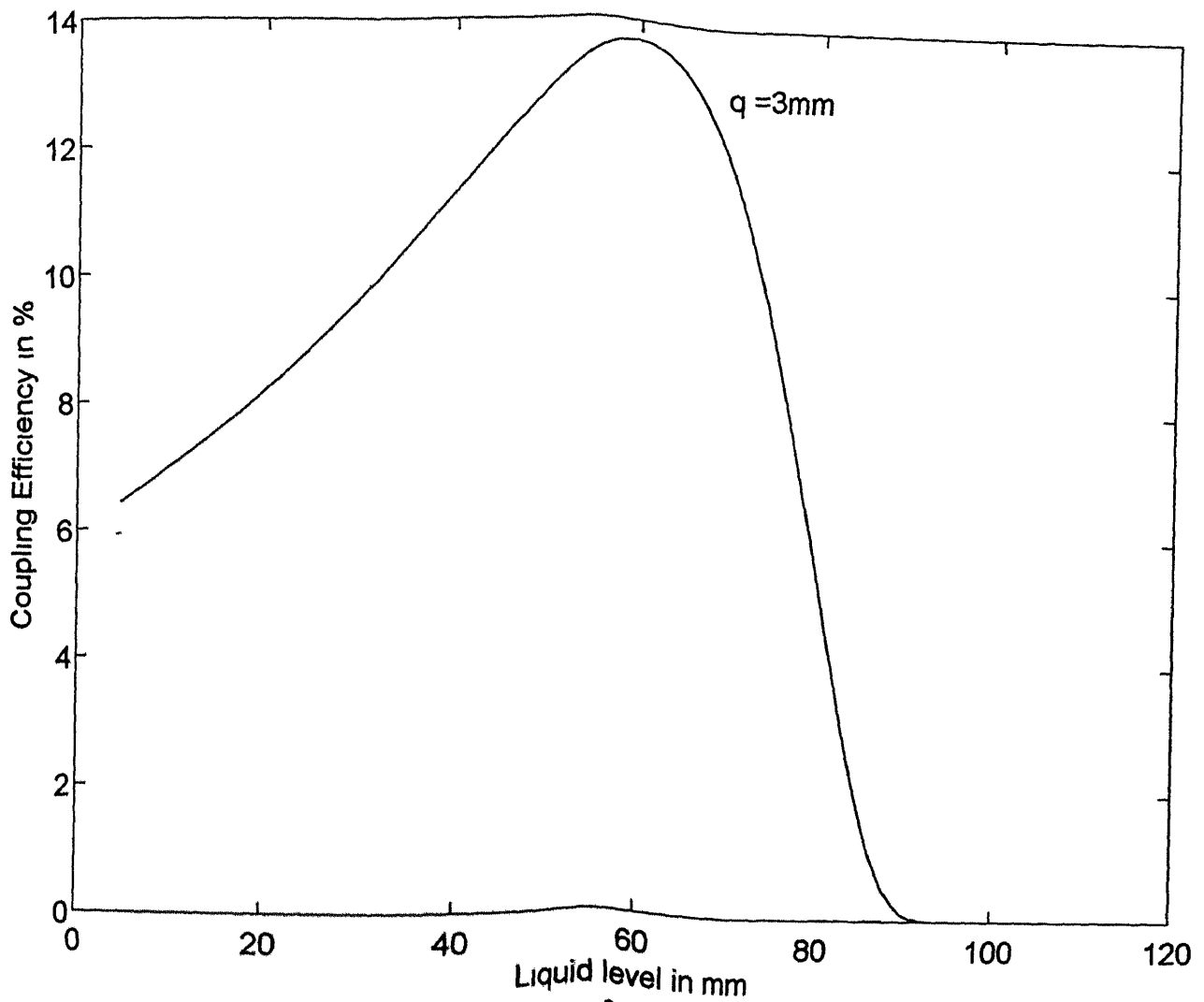


Fig. 6.3 Coupling Eff vs. Liq. level for Sensor Configuration No. 3, offset  $q = 3\text{mm}$

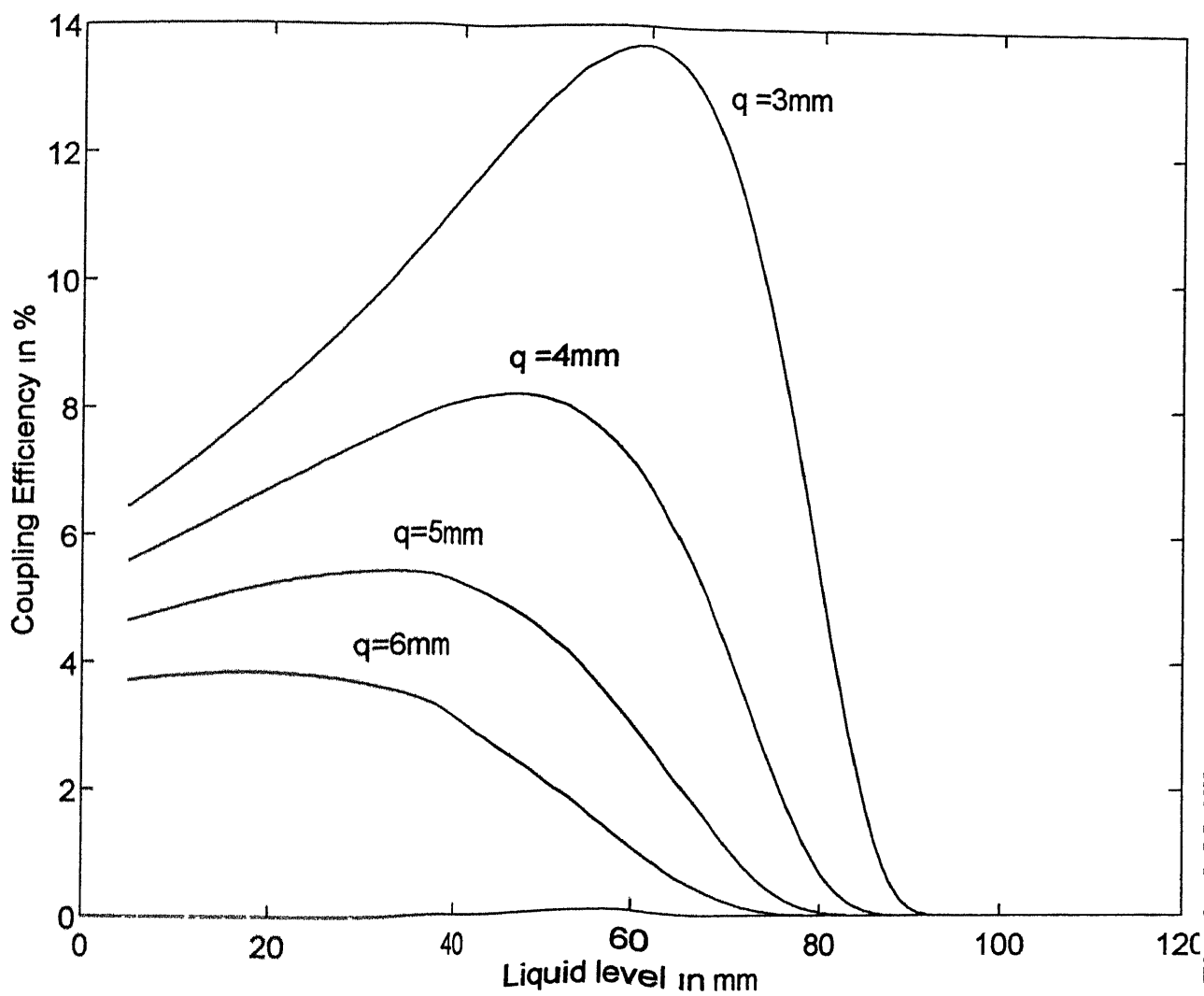


Fig 6.4 Coupling Eff vs Liquid level for variation in the offset  $q$

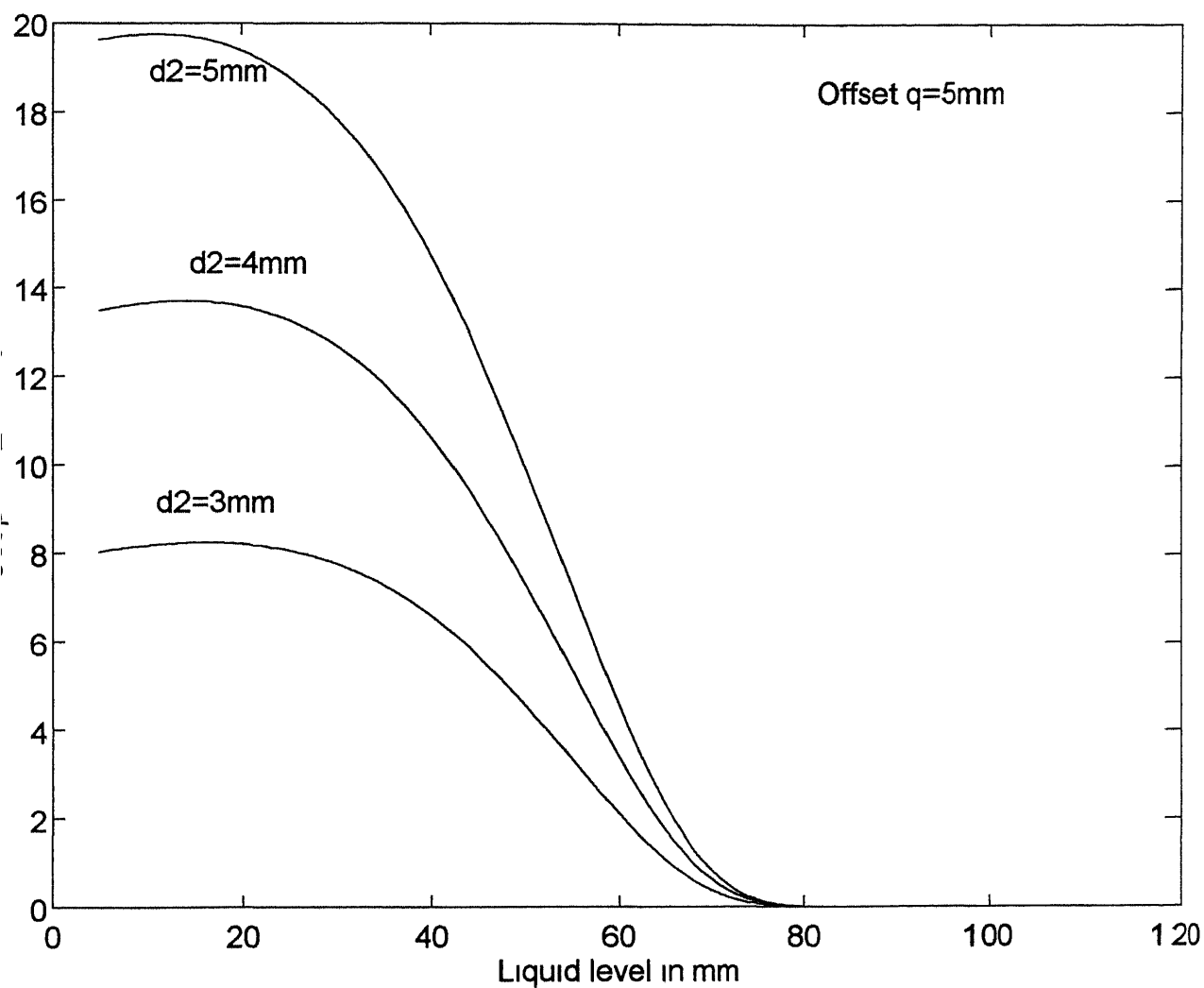


Fig 6 5 Coupling Eff vs Liq level, for variation in radius of detector

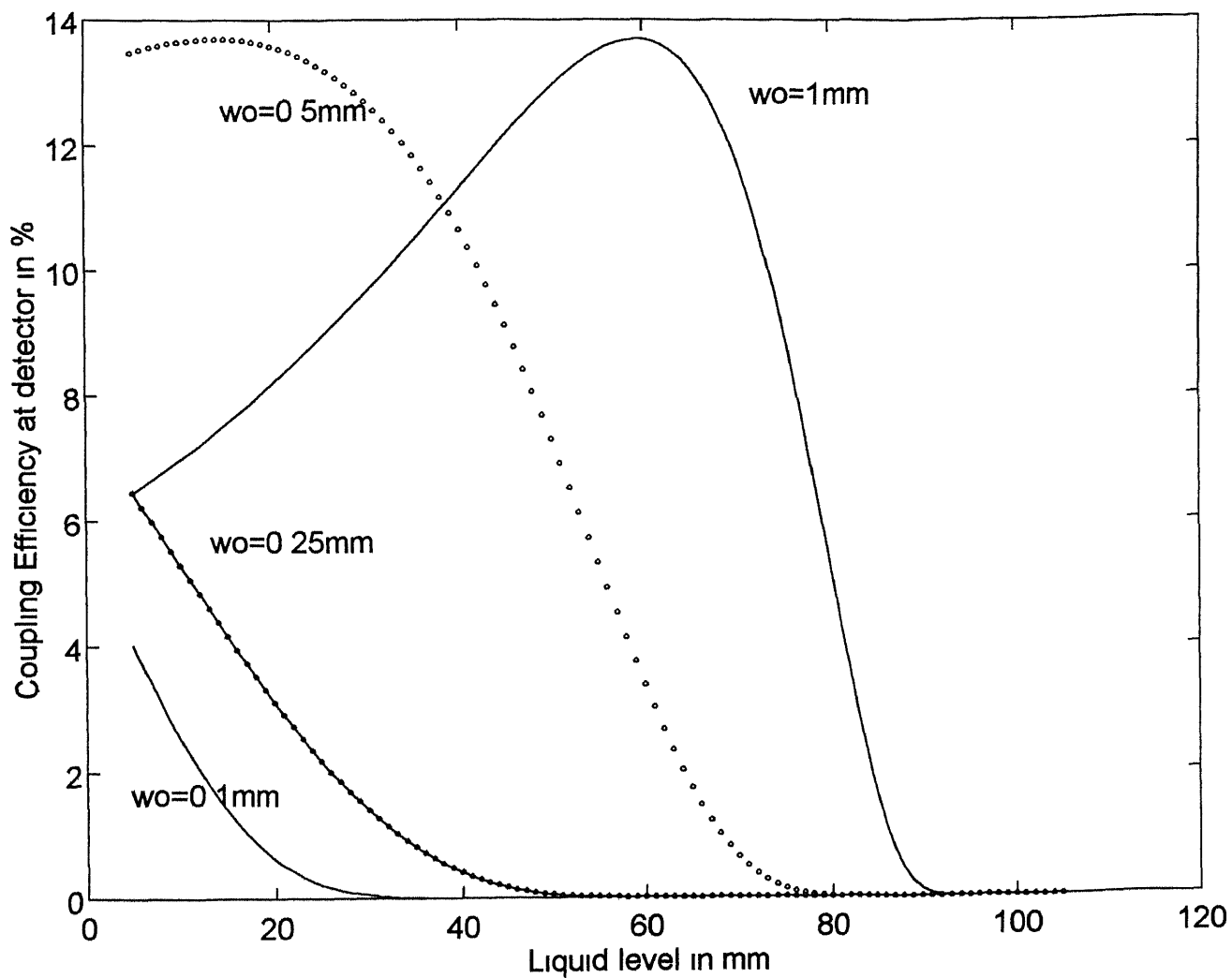


Fig 6 6 Coupling Eff vs Liq level, for variation in min spot size

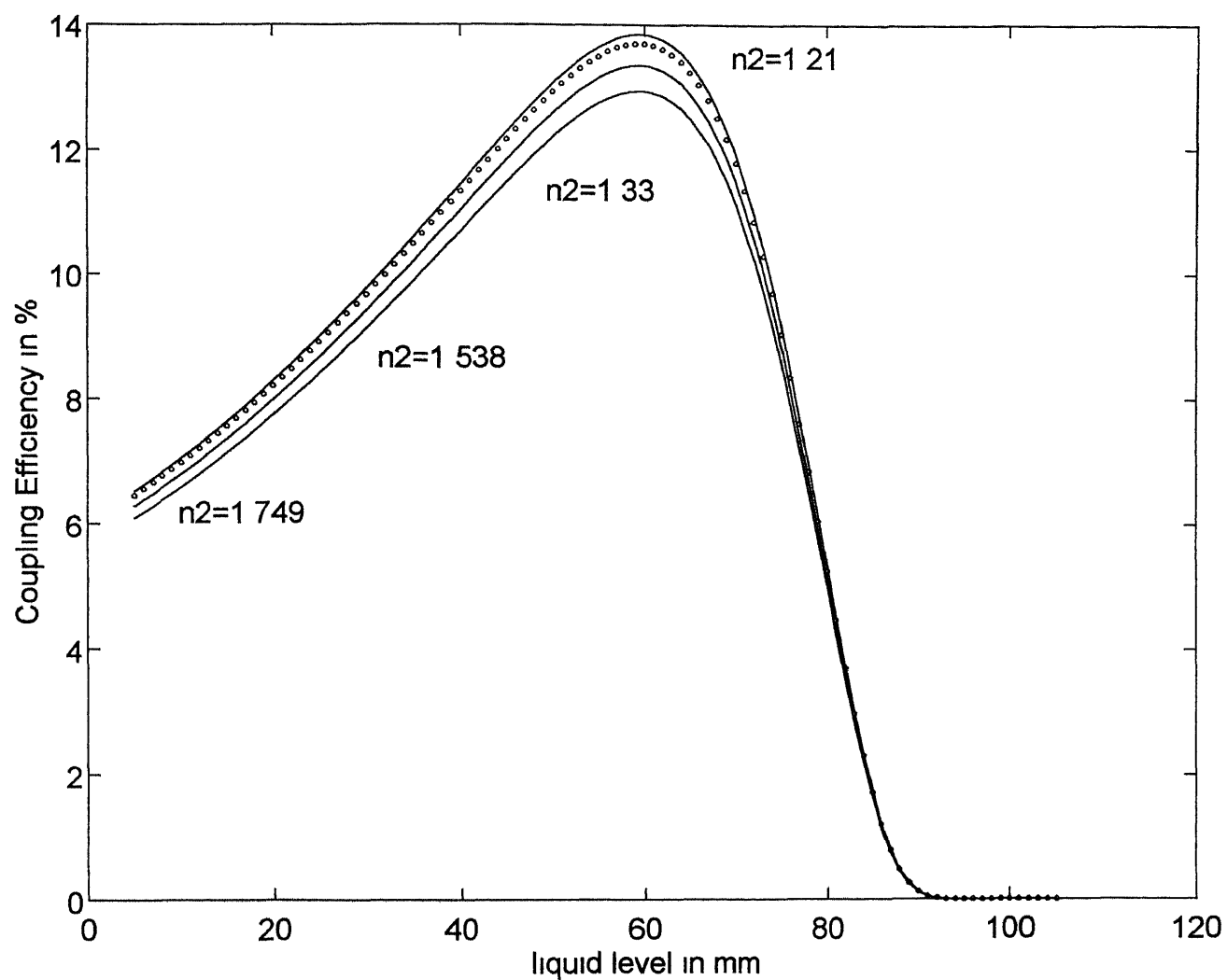


Fig 6 7 Coupling Eff vs Liq Level, for variation in liq refractive index

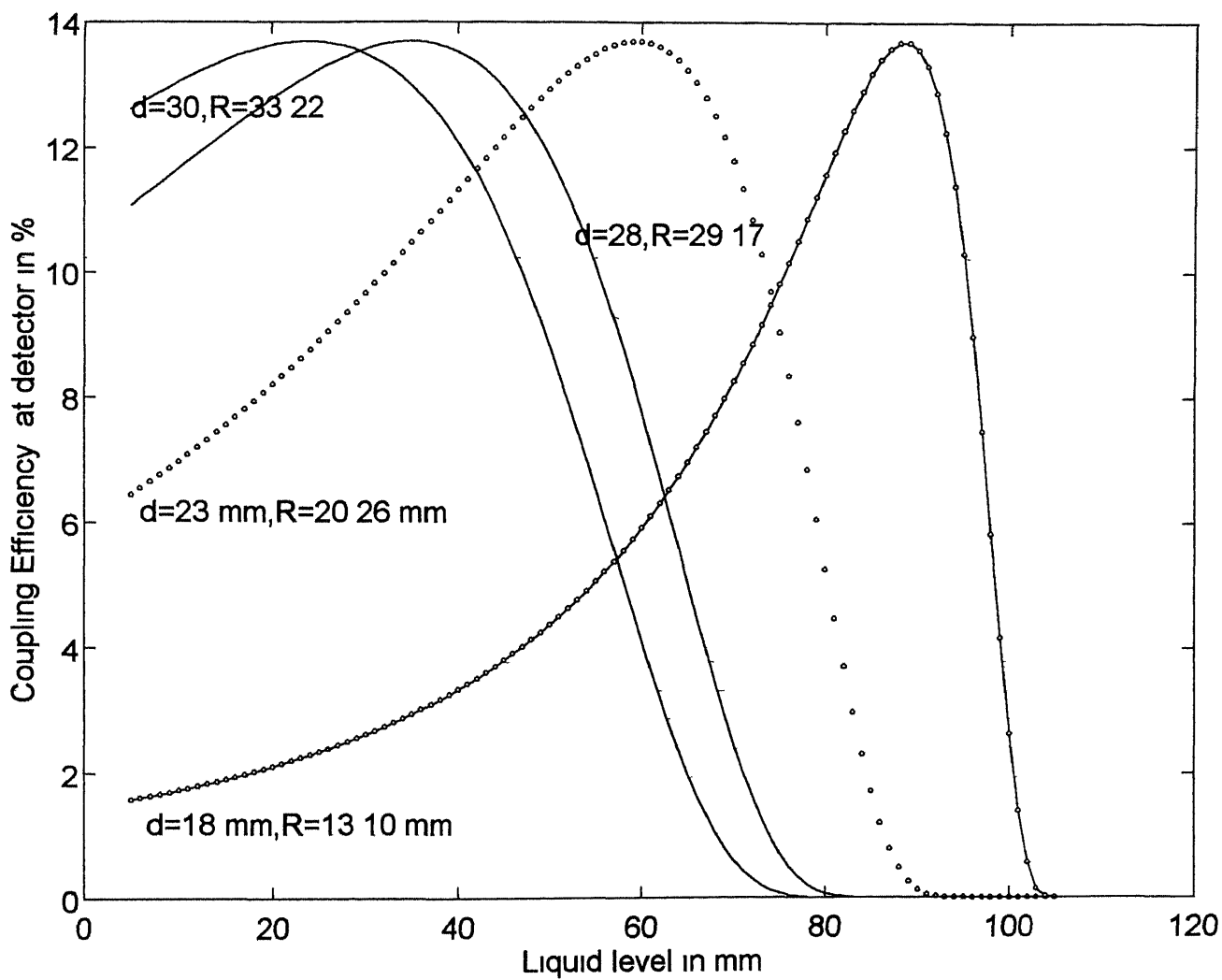
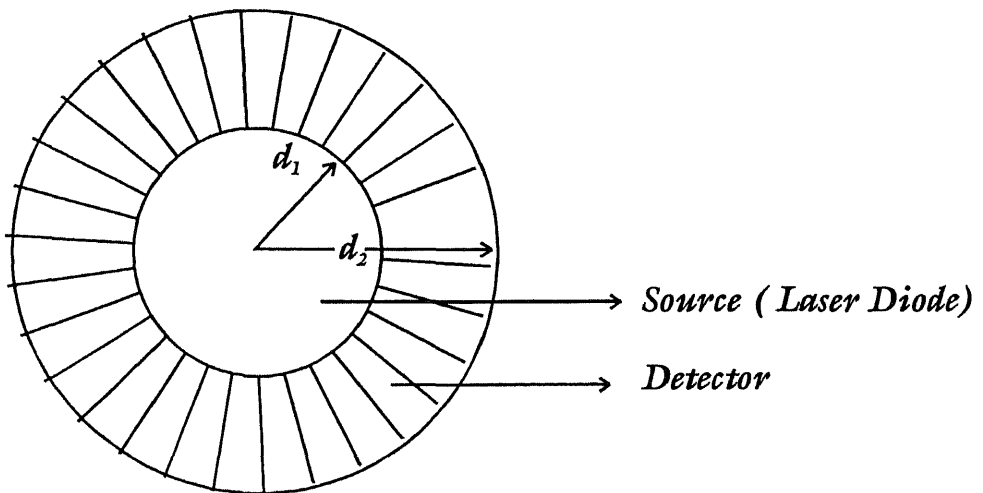


Fig 6 8Coupling Eff vs Liq Level, for variation in diameter of tube

**LEGEND**

$d_1$  = Radius of source  
(& inner radius of  
annular detector)

$d_2$  = Outer radius of an  
annular detector



**Fig. 6.9** An annular(ring shaped)detector

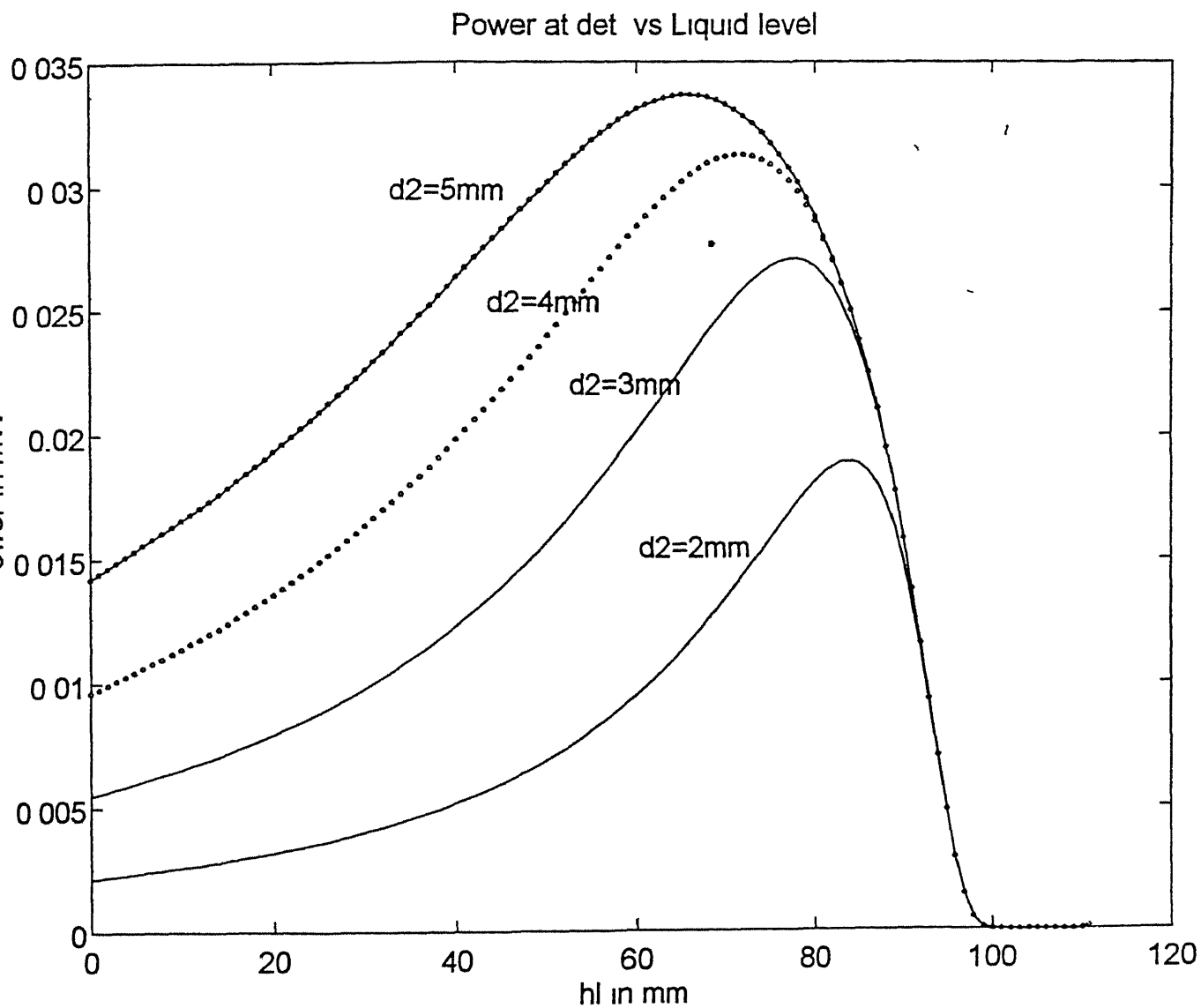


Fig 610 Power vs Liq level, for variation in outer radius of ann det

## SCOPE FOR FUTURE WORK and CONCLUSION

### 7.1 Conclusions

The package design for a low cost liquid level optic sensor has been studied in detail using the geometric optic and physical optic considerations. The expressions for the spot size at the detector and the power coupled to the detector, have been derived for the simple case of all the four possible configurations of our optical liquid level sensor. A comparative analysis of the four configurations was carried out and a feasible configuration for our low cost optical sensor was selected and analyzed in detail.

The design parameters were varied and the following were observed:

The effect of various parameters on the sensor response are seen and analyzed for better understanding of the behaviour of the optical sensor. It is seen that coupling efficiency increases with an increase in the radius of the detector, because larger area at detector is available for collection of power. Thus one way to improve coupling efficiency in an optical sensor is by selecting a large size detector.

(a) It is also seen in configuration no 3, that power initially increases with increase in liquid level and then decreases after reaching a peak value because after a certain liquid level, when the light reflected from the liquid surface falls on the complete area of the detector, then maximum  $P_d$  and Eff are achieved. After this stage, though there is no further increase in the area of the detector which receives light, yet the intensity of light falling per unit area decreases and thus  $P_d$  and Eff decrease and this is the region of back slope of the plot.

The variation in the response of this sensor is uniform and both the front and the back slope can be utilised for sensing purpose. However, when the front slope is used for sensing, the dead zone that occurs is different than the dead zone that would occur if the back slope is used for sensing.

(b) The values of various design parameters for our optical liquid level sensor were selected after a detailed analysis and the list of the same is given at table 6.1.

(c) The offsetted detector has a dead zone beyond 85 mm and as such accurate level sensing is not possible from 85 mm to 105 mm.

- (d) The drawback of the offsetted detector listed at srl (c) above can be overcome by using an annular detector, which is able to sense upto 100 mm
- (e) The annular detector is not prone to misalignment errors and is thus more reliable than the offsetted detector
- (f) The physical offset between the source and the detector for the reflective type of sensors has been incorporated in the calculations for the spot size, power and coupling efficiency. It is seen that as offset increases, efficiency decreases as less power is being coupled to the detector because the detector falls partially within the cone of light reflected from the liquid surface
- (g) In view of the nature of propagation and spread of the gaussian beam, in order to minimize reflections from the side walls, an ideal shape for the low cost optical sensor of configuration no 3 is a tube which increases in diameter on going from the top to the bottom of the tube

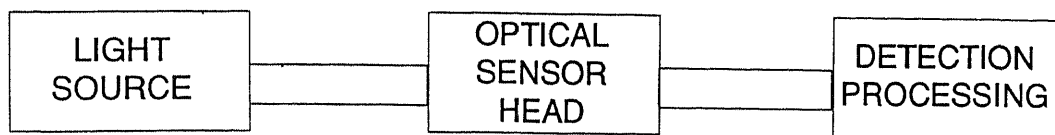
## 7.2 Scope for Future Work

**7.2.1 Various Applications Possible** In this thesis we have looked at a reflective optical sensor for a reflecting surface with a radius of curvature 'R'. This work has a large application in automobile and aeronautical industry. The same work can be used for measurement of various kinds of lateral displacement.

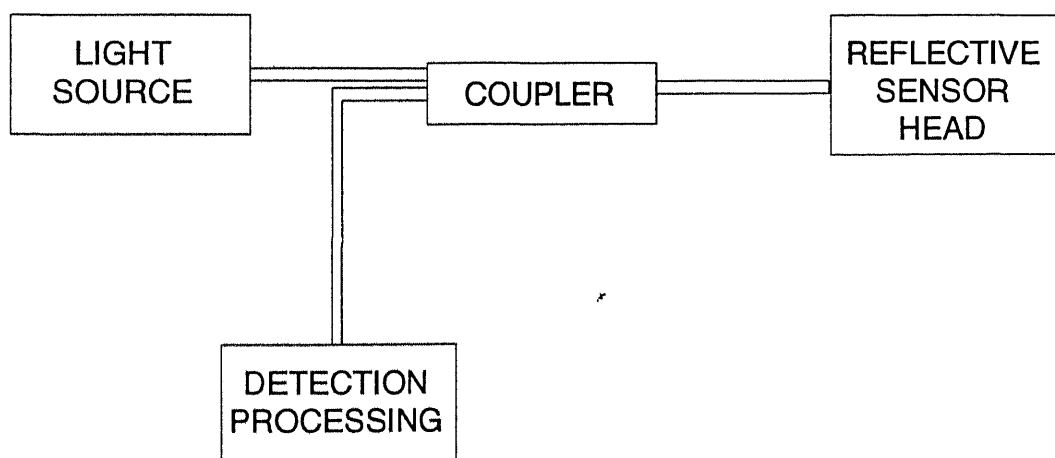
Based on the work done in this thesis, the transmissive type of sensor can be used to measure the refractive index of the liquid.

Other than liquid level measurement, the work done in this thesis can be used for vibration measurement. The light can be made incident on a reflecting diaphragm and the number of vibrations is equal to the frequency of change of the radius of curvature of the diaphragm, which can be measured. The same principle can be extended for the design of sound intensity hydrophones and in SONAR applications.

The same work can also be extended for various cylindrical objects having circular reflecting surfaces, thus shaft wear out can be measured using these principles.



**(a) TRANSMISSIVE MODE**



**(b) REFLECTIVE MODE**

**FIG. 7.1 Extrinsic Fiber Optic Sensors**

**EXPRESSION FOR SPOT SIZE AT DETECTOR FOR CONFIGURATION NO 1**

In this configuration , the laser diode is at the top of the tube and the detector is at the bottom As shown in Fig ( 5 5 ) , if some liquid of refractive index  $n_2$  partially fills up the gap of length  $z$  between the optical source and photodiode , then the optical beam will propagate partially through air (distance  $z - h$ ) and partly through a liquid column of height  $h$  The light travelling from the top of the tube thus encounters a concave dielectric interface whose ray matrix in terms of A,B,C,D parameters [ 7 ] is given by

$$\begin{bmatrix} 1 & 0 \\ \frac{(n_2 - n_1)}{n_2 R} & \frac{n_1}{n_2} \end{bmatrix} \quad (A 1)$$

The detailed derivation of the above expression has been done in appendix B In the above expression ,  $R$  is the radius of curvature of the liquid ,  $n_1$  and  $n_2$  are the refractive indices of air and liquid respectively

The complex beam parameters at various planes are as under [5]

$q_1$  - at plane 11' i.e at the output of the laser diode

$q_2(-)$  - at plane 22' i.e above the air liquid interface ( as viewed from the top of the tube )

$q_2(+)$  - at plane 22' i.e below the air liquid interface ( as viewed from the top of the tube )

$q_3$  - at plane 33' i.e at the input end of the detector

At plane 11' that is at source ( $z=0$ ) , the complex beam parameter  $q_1$  is given by [6]

$$1/q_1 = -j \lambda / n_1 \pi w(z)^2 \quad (A 2)$$

where  $w_0$  is the size of gaussian beam measured at  $z=0$  The transformed beam parameter  $q_2(-)$  just to the left of the air liquid interface is given by  $q_2(-) = q_1 + (z - h)$  The beam parameter  $q_2(+)$  , just below the air liquid interface is given by

$$q_2(+) = \frac{Aq_2(-) + C}{Bq_2(-) + D} \quad (A 3)$$

where A, B, C, D are the elements of the ray matrix given by expression (A 1)

For the ease of computation we will denote  $M = n_1 \pi w(z)^2 / \lambda$  (A 4)

and  $Q = (n_2 - n_1) / n_2 R$  (A 5)

$$\text{thus } q_2(+) = \left[ \frac{jM + (z - h)}{Q(jM + z - h) + (n_1 / n_2)} \right]$$

Finally the beam parameter  $q_3$  at the liquid detector interface is given by  $q_3 = (q_2(+) + h)$

$$\text{Thus } q_3 = \left[ \frac{jM + (z - h) + Qh(jM + z - h) + h(n_1 / n_2)}{Q(jM + z - h) + (n_1 / n_2)} \right] \quad (\text{A } 6)$$

Also,  $q_3$  is related to the beam spot size  $w_3$  and radius of curvature of the beam  $R_3$ , through the equation

$$1/q_3 = 1/R_3 - j \lambda / n_2 \pi w_3^2 \quad (\text{A } 7)$$

From equations (A 6) and (A 7), comparing the coefficients of the imaginary terms, the expression for beam spot size at plane 33' given by

$$w_3 = w_0 \sqrt{(1 + (n_2 - n_1)h / n_2 R)^2 + (g \lambda / n_1 \pi w_0)^2} \quad (\text{A } 8)$$

where  $g = ((n_2 / n_1)h / n_2 R + 1)(z - h) + (n_1 / n_2)h$

## RAY MATRIX FOR A CONCAVE DIELECTRIC INTERFACE

1 Shown in fig B 1 ,  $\theta_1$  and  $\theta_2$  are the angles made by the incident and the refracted rays with the normal to the surface

2 The following conventions are followed

- (a) Light travels from right to left
- (b) Angle is positive if upward sloped
- (c) Height is positive (i.e.  $+x$ ) if measured above the optical axis
- (d) Distances along optical axis are measured with respect to the vertices
- (e) Distance travelled along direction of light is positive

By snells law ,  $n_1 \sin \theta_1 = n_2 \sin \theta_2$

Thus  $n_1 \theta_1 \approx n_2 \theta_2$

$$|\theta_1| = |\psi| - \alpha_1 \quad \text{where } \psi = \tan^{-1} x_1 / R \approx x_1 / R$$

$$\text{Thus, } |\theta_1| = (-x_1 / R) - \alpha_1$$

$$\theta_2 = |\alpha_2| + |\psi|$$

$$\theta_2 = -\alpha_2 - \psi \quad (\text{because of sign convention})$$

$$\text{But } n_1 \theta_1 = n_2 \theta_2$$

$$n_1 (-\psi - \alpha_1) = n_2 (-\alpha_2 - \psi)$$

$$\Rightarrow n_2 \alpha_2 = n_1 + (n_1 - n_2) \psi$$

$$\Rightarrow \alpha_2 = ((n_1 - n_2) / n_2) (-x_1 / R) + (n_1 / n_2) \alpha_1$$

$$= ((n_2 - n_1) / n_2 R) x_1 + (n_1 / n_2) \alpha_1$$

$$\& x_2 = 1 x_1 + 0 \alpha_1$$

$$\text{Thus } \begin{bmatrix} x_2 \\ \alpha_2 \end{bmatrix} = \begin{bmatrix} 1 & 0 \\ (n_2 - n_1) / n_2 R & (n_1 / n_2) \end{bmatrix} \begin{bmatrix} x_1 \\ \alpha_1 \end{bmatrix}$$

$$\text{Thus the ray matrix is given by the expression } \begin{bmatrix} 1 & 0 \\ \frac{(n_2 - n_1)}{n_2 R} & \frac{n_1}{n_2} \end{bmatrix}$$

# **LEGEND**

*inc* = incident ray

*ref* = refracted ray

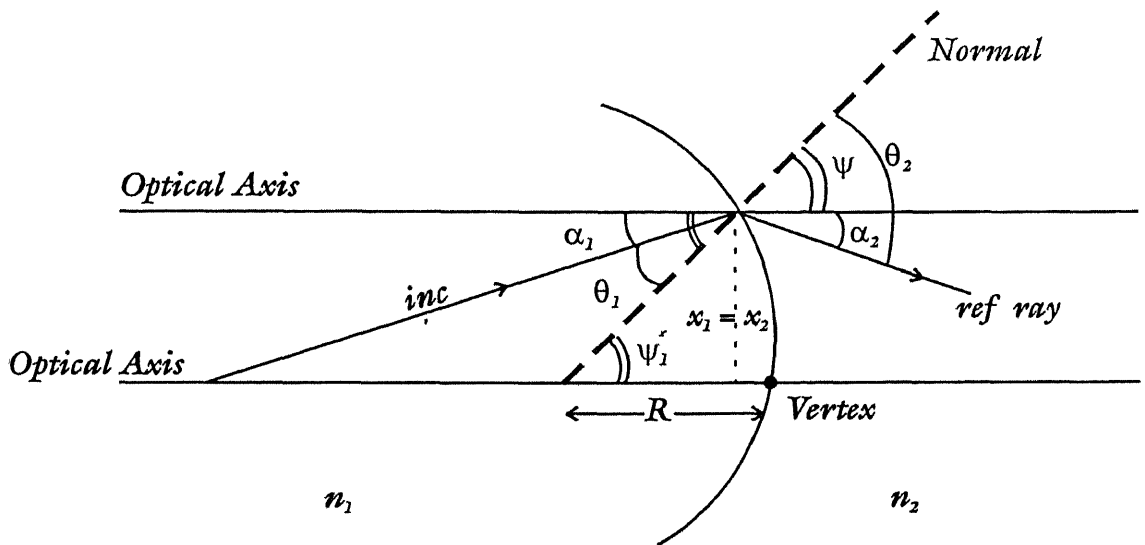


**Fig. A.1 Concave spherical dielectric interface**

15

**121848**

Date Slip **127828**

This book is to be returned on the  
date last stamped

[illegible]